Reviewers' comments are colored in black, authors' responses are colored in blue.

General remarks

We would like to thank both reviewers for the time and effort they invested in reviewing and assessing the manuscript. Both reviewers have pointed out that we do not propose a solution to the suboptimal performance of a controller tuned for flat terrain in complex terrain. The contribution is not in developing new models or methods, but in analyzing an existing method (k-ω^2 control) from a new perspective and at a high level of numerical and analytical detail. Since k-ω^2 control is widely used, we believe this work significantly contributes to the wind energy research community's knowledge.

We have made significant changes to the manuscript, with the most relevant listed below. None of the modifications affects the article's conclusions.

- The title has been changed to *"Aerodynamic analysis of standard variable-speed torque control in complex terrain,"* to clarify the scope of the article.
- The identification of the maximum performance at the different turbine locations has been improved by replacing interpolation on a coarse λ-θ grid to find the optimum by a nested grid search where the optimum is found as a discrete value on a grid with spacing $\Delta\lambda = 0.02$, $\Delta\theta = 0.02$ deg. This modification did affect numerical values in the manuscript, but the conclusions stayed unaltered.
- The introduction was rewritten with a greater focus on prior studies and on the specific contributions of this work to the authors' prior publications. Furthermore, the description of the controller has been mostly moved to the methodology section, with only a brief description remaining in the introduction.
- The methodology now features more details on the grid sensitivity (Sect. 2.6), as well as a section on the controller (Sect. 2.2). More explanations of the methodological choices are also provided.
- Flow fields are now included in the manuscript. In this context, also the expected performance biases due to different levels of turbulence intensity are analyzed (Sect. 3.1).
- Throughout the results section, the simulation results for the additionally considered cases (C2, C3.X, C4.X) are now shown as well.

Since the modifications are significant, we kindly ask you to review the entire, revised manuscript.

Reviewer 1

The manuscript in question presents simulation results and analysis regarding the performance of standard k-omega-squared torque turbine torque controllers in non-flat terrain. Although by itself an interesting and relevant topic worthy of publication in WES, I believe the manuscript has some significant shortcomings that would need to be addressed before it can be published here. All comments can be found in the PDF attached, but my main concerns are reiterated below:

- The paper is generally poorly written. Some sentences are hard to understand or do not flow naturally. The structure of the paper does not always make sense and should be reconsidered. The introduction is missing big chunks of information that are relevant for the paper. I strongly suggest having a professional editor or at minimum a native English speaker with writing experience take a look at the manuscript before resubmitting.
  We carefully proofread the entire manuscript and hope that the new submission now satisfies the reviewers' language standards.
- The authors generously self-cite previous work, but fail to point out what specifically this manuscript adds with respect to previous publications. I have not read all the previous publications in full, but I've read enough to know that there is significant overlap between those papers and this

manuscript. To address this, the authors should include a more descriptive paragraph on previous research in the introduction, followed by a summation of contributions unique to this work.
We have added a paragraph at the end of the introduction clarifying the contribution of the present work beyond our previous studies.

- A lot of the methodological choices and modeling simplifications are not or not well explained or justified. This includes but is not necessarily limited to: the choice of the terrain, the choice of the surface roughness, the choice of the turbine location, the choice of the controller used, the choice of the turbine model. Flow results from the RANS simulations, which are the heart of the manuscript, are almost completely omitted, making it very hard for readers to assess what is happening to the flow around the hill, with and without a turbine.
We have extended the description of the methodological choices. Furthermore, flow results with and without the turbine are now included in the manuscript.

- From the introduction, I was made to understand that the main contribution of this manuscript was that it investigates how suboptimal control affects power performance of turbines in non-flat terrain. The authors cite different studies investigating complex terrain, and note that suboptimal control might influence the findings of these studies. However, in the manuscript, they fail to quantify the exact influence of a sub-optimally tuned controller on the total power production of a turbine on or near a hill. Furthermore, they fail to implement potentially simple improvements to the controller, to verify that the power production can actually be increased on non-flat terrain.
We added numerical values of the suboptimal performance of the controller. As stated earlier, the goal of this article is not to propose a new control method. However, as also noted in the article, a simple solution to the suboptimal performance is to retune the torque constant k (and adjust the blade pitch), which would restore optimal operation. The C_P-λ curves in Fig. 6 in the revised manuscript show that performance can indeed be increased by such a retuning. However, we did not perform simulations with a retuned controller because, based on the generated insights that the controller strictly follows its control curve, we can already conclude that this would help.

Despite these shortcomings, I believe this manuscript still has the potential to be published in WES. Apart from improving the presentation quality, this would also require a significant rewrite to emphasize the value of the manuscript with respect to previous work, as well as additional simulations to assess the true influence of sub-optimal or uncalibrated control on wind turbine power production in non-flat terrain. Ideally, the manuscript would also propose a solution to this challenge (perhaps as simple as a recalibration of the optimal TSR), including simulations showing the potential benefit of this solution.

In the following, comments from the manuscript attached by the reviewer are answered. Comments regarding grammar and style are not listed, as their suggestions are directly included in the revised manuscript. Thus, only comments that, from the author's perspective, require a direct, formal response are discussed below.

Line 7 f. These numbers are misleading as they are with respect to the reference wind speed. You should decouple which part of the performance loss is due to the hill, and which part due to the controller.
We improved the phrasing and explicitly state the reduction of the power coefficient due to the suboptimal operation of the controller.

Line 16 In my opinion, the introduction requires a significant rewrite. The order of things is not logical, parts are not well-written, and an introduction to the effect of complex terrain on the flow is missing. I suggest ordering the introduction as follows: 1) introduction to flow in flat terrain, and how controllers are tuned for optimal performance in these conditions 2) introduction to complex terrain and how it influences airflow 3) Overview of literature studying turbine performance in complex terrain, showing the knowledge gap that you are addressing with this paper 4) Introduction to your proposed solution
We have modified the introduction and also have incorporated your suggestions.

Line 22 I disagree with the causality here. In Region 2, the controller aims to extract maximum power, which HAPPENS to coincide with a (relatively) constant CP and CT. Not the other way around. The controller in this region generally regulates torque to keep the TSR constant, so perhaps you meant to say that

From our perspective, it is not a coincidence that C_P and C_T are constant in region 2. When a turbine controller is designed, a C_P-TSR-pitch surface, as shown in Fig. 4 of the revised manuscript, is consolidated to identify the point at which the turbine performs aerodynamically optimally. The TSR and pitch at the optimum C_P are then used to set the blade pitch and the torque constant (Eq. 3 in the revised manuscript), which are subsequently used to calculate the generator torque. Fixing TSR and pitch ensures constant local flow angles at the blade and performance at the C_P these values correspond to, regardless of the wind speed. This can be seen in Eqs. (3) and (7) of the revised manuscript. The entire derivation of a generator torque controller is based on the assumption that there is only one distinct point of optimal operation (TSR, pitch) at which the maximum power performance quantified by the optimal C_P is reached. So yes, the controller attempts to keep TSR constant, but only because at this TSR, the C_P is optimal. See also Johnson et al. (2006) and Bianchi et al. (2007). Thus, it is not a coincidence that C_P is constant in region 2. For C_T, the argument can be made that forces scale with the wind speed squared (at constant TSR and pitch), so the ratio of force to wind speed squared must remain constant. So it is a consequence of the design, and one could potentially argue it is a coincidence. However, because a C_T-TSR-pitch surface uniquely relates a given TSR and pitch to a given C_T, one could also speak of a deliberate decision to operate at this C_T. These arguments, of course, only hold when Reynolds-number independence at the blades can be assumed. We have also improved the description of the torque controller in the revised manuscript and hope it further clarifies it.

Figure 1 I believe this figure is redundant. The different control regimes of a turbine can be considered general knowledge, so unless you use data specifically extracted from this figure later in the paper, this can be omitted and the text describing the regions suffices (with potentially a reference to the original source of this figure)
We have removed Fig. 1 from the original manuscript and instead added Fig. 5 in the revised manuscript, which not only shows the different control regions, but also the impact of the different turbine positions on the power and control curves.

Line 28 What I'm really missing here is an introduction to complex terrain / topology and the effect it has on the wind. Explain that most WTC research focuses on "simplified" situations with flat/uniform terrain, and how the flow generally develops around a turbine in this terrain. Then introduce complex terrain and explain what effect that has on flow development. Then, finally, you can argue why this affects power extraction and might require turbine control redesign
In this work, we focus on a situation that is complex enough to represent a certain terrain-induced effect, namely, flow acceleration and deceleration, but not too complex so that no clear conclusions can be drawn anymore. Therefore, we do not perform an in-depth literature review of the flow in complex terrain. It would touch up on many topics, such as stability, thermal winds, and more, without adding much to the specific problem we are interested in. Nonetheless, we have addressed your concern by including how controllers are usually tuned, considering only streamwise uniform flow and further argue why in complex terrain this tuning might not be sufficient (see l. 29 ff.).

Line 34 I'm not sure I understand this statement. The controller will do what it's made to do, regardless of the flow. Non-uniformity in the flow just acts as a disturbance. I think what you mean to say (or should say) is that the effect of complex terrain on the flow might fall outside the design scope of the controllers implemented in these studies, and as such, controller performance might be suboptimal.
We have clarified this sentence (see l. 60 ff.).

Line 40 This part (lines 40-60) might be to technical for an introduction. Consider moving to Section 2, and limit yourself to explaining the assumptions made in turbine controller design, and why these don't apply in complex terrain.
We have moved most of the technical description of the controller to the methodology (Sect. 2.2) and only kept what we consider as relevant for the reader in the introduction.

Line 71 So no alternative controller tuned for complex terrain will be introduced in this paper?
No alternative controller is introduced as we consider it as out of the scope of this study, which focuses on the physical analysis of the k-ω^2 controller.

Line 77 Why were these three cases chosen specifically? For example, why wasn't a case with the

turbine behind the hill considered? I would expect different performance there too, right?
Indeed, behind the hill, we would also expect a different performance. The cases in this work are considered due to the following reasons: Flat terrain is used as a reference case; the case ahead of the hill is chosen because it features a situation where flow acceleration leads to a higher performance than in flat terrain, while the case on top of the hill leads to lower performance due to the deceleration. So we have one case with higher performance and one with lower performance than expected. We have added this explanation in l. 88 ff. in the revised manuscript.

Line 84 Only the blade geometries, or just the full geometry (tower, nacelle, hub, etc)?
Only blade geometries are considered. In the revised manuscript l. 95 clarifies this now.

Line 86 While I agree that the k-omega-squared controller is the most common way to regulate torque in region 2, it is not the only way. For example, the Reference Open-Source Controller (ROSCO) also offers the option to use TSR tracking based on internal wind speed estimates. I would expect these estimates to go up at the bottom of the hill or go down at the top of the hill, which might result in closer-to-optimal performance for this controller. Comparing results only for the most basic torque controller is in my opinion not a fair way to determine potential power losses due to complex terrain
As pointed out by the reviewer, the k-ω^2 controller is the most common way of wind turbine control in region 2. Therefore, it is in our perspective consequent to also use this controller in our analysis. We can only speculate how a TSR-tracking controller would affect power performance, and a future study (potentially based on transient simulations) should certainly compare different control strategies. The focus of this study is on understanding the k-ω^2 controller in detail.

Line 102 I would like to get a better sense of what the inflow wind in the simulations looks like. Is wind shear considered/implemented here? I can imagine that this also has an effect on the flow of the turbine on the top of the hill, as it will likely experience higher wind speeds than the turbine at the bottom of the hill. Please include (averaged) wind speed and turbulence (and possibly wind direction) plots as a function of height, possibly at different locations in the domain (inflow boundary, location A, B, C). I think this is absolutely vital information to assess the results presented in Section 3.
Figure 3 in the revised manuscript shows the undisturbed vertical velocity and turbulence intensity profiles at the turbine positions. Since the inflow is quasi-two-dimensional, a wind direction plot is not necessary, and the domain inflow profile is given for all cases by Eq. (12) in the resived manuscript.

Line 117 Why was this configuration chosen? Is there any reason/logic to this configuration? How does this compare to other complex terrain studies? How realistic is this configuration with respect to actual hills that might have wind turbines placed on/nearby them?
The reason for this setup is that it allows for easy modification of the flow around the turbine by modifying hill and surface parameters. As mentioned before, the terrain is complex enough to fall outside regular turbine design considerations, but not so complex that it is not possible to draw definite conclusions. Thus, the goal is not to achieve a highly realistic setup. In general, the setup's dimensions are similar to those in other studies (Liu and Stevens, 2020; Mishra et al., 2024; Troldborg et al., 2022). This is also elaborated in Sect. 2.4 of the revised manuscript. How this setup compares to realistic conditions is a very open question, given the variety of complex terrain. There are certainly cases where it compares well, see, for example, the wind turbine located on a landfill in Freimann, Munich, Germany.

Line 129 The ADM is a significant simplification of a real turbine rotor. Have the authors also investigated what effect using such a simplification has on the results? E.g., by comparing results with an actuator line model? Especially in non-uniform conditions, I can imagine that you might get very different results.
We have not compared the results to actuator line models as we are performing RANS simulations. However, we do not expect the main conclusions to differ significantly, as they are supported by theoretical considerations in the discussion and the appendix. In an earlier study by Hodgson et al. (2021), comparing actuator disk and actuator line models coupled with the aeroelastic solver Flex5 (Øye, 1996)(which includes a torque controller), it was found that steady-state performance and loads agreed well between the methods. Nonetheless, unsteady simulations might yield additional insights into unsteady effects, and actuator line modeling is a logical next step in our research.

Line 134 "in this work" implies that these results will be shown later on, which I do not believe is the case. I do appreciate that the authors took the time to execute such a sensitivity analysis, but would like to see the results in a little bit more detail. Perhaps you could show how the cell volume affects the power and induction in a simple plot?
We have added Fig. 2, which shows the sensitivity of reference velocity and C_P on the cell size.

Line 156I understand that RANS simulations can be expensive, but this is a very coarse grid. The differences in the optima found are smaller than the applied grid size in cases A and B. I would say it is prudent to reduce the grid size around the optimum to increase the reliability. At the very least, you should run simulations with the found optima to verify that the CP values found through interpolation hold. Perhaps that is already done, but if so, that is not clear from the text
We have modified the methodology and identified the points of maximum performance now by a nested grid search with the finest grid having a spacing of $\Delta\lambda = 0.02$, $\Delta\theta = 0.02$ deg. This allows for making definite conclusions about differences in power between the considered cases.

Line 158 Please clarify. Furthermore, the same seems to be the case for labda = 9, theta = -5
The comparably high thrust coefficient accompanied by a strong deceleration behind the hill leads to an oscillating solution. See l. 241 ff. in the revised manuscript. The case for $\lambda = 9$ and $\theta = -5$ indeed converges, but in the original figure (Fig. 2 of the original manuscript), the colormap was cut off at a value above the achieved C_P for this case, so it was not directly visible in the figure. The new figure (Fig. 4 revised manuscript) has an improved colormap.

Figure 2I think you should split this figure up into two figures: a first figure showing the topology, including more details on the slope angle, incline, horizontal and vertical distances, etc. And a second figure that shows the CP surfaces for the three different locations.
The figure is split up in Fig. 2 and Fig. 4 in the revised manuscript.

Figure 2 In addition to this figure, I would love to see a figure of the wind speed (both disturbed and undisturbed by the turbines) as a function of horizontal location, either at hub height (so moving along the surface of the ground) or at a specific altitude (not moving along the surface of the ground), to get a better understanding of the influence of the terrain on the flow
Figure 8 in the revised manuscript shows the undisturbed and disturbed wind speed at constant height (hubheight) above ground.

Line 180 I would like to see the difference between performance with the "standard" controller (which I assume will use a pitch of 0 degrees) and the calibrated controller. I assume that the difference in performance is significant, perhaps even bigger than the difference between cases A, B, and C, which shows that your simulation environment and model assumptions have perhaps a bigger influence on the performance of the controller than the terrain does.
We have performed the same set of simulations using the control constants specified by Bak et al. (2013) with $\theta = 0$ deg and $k = 10652234\ \mathrm{Nm}^2$. Note that k is adjusted for the generator efficiency. Results are shown in Fig. 1. In comparison with Fig. 6 of the revised manuscript, the following can be said: In general, for $\theta = 0$, significant differences in maximum performance between the considered locations can be identified. At the hill foot, the maximum performance is approximately 2.2 % higher than in flat terrain and on top it is approximately 17.5 % lower. These values are smaller than what we find for our tuned controller (2.5 %, 18.7 %). However, it is also known that the effect of streamwise flow acceleration on performance increases with increasing C_P, which is higher in the tuned case (Zengler et al., 2024, 2025). Using the original control settings yields non-optimal performance and a different C_P compared to Bak et al. (2013) in flat terrain in our case, because the flow representation in CFD differs from that in BEM (which was used to tune the original controller). This effect is also visible in other studies (Hodgson et al., 2021). On top of the hill, the difference between the performance at which the controller settles and maximum performance seems to be comparably small; however, the control curve reveals that this is because the control curve is not crossing the optimum in flat terrain. If this were the case, differences in performance on top of the hill would be more significant. Also in this case, the controller operates even further away from the optimum on top of the hill.

There is a fundamental problem when adapting control values from BEM to CFD: one can either use the torque constant directly or use the tip-speed ratio to retune the controller and then obtain the torque

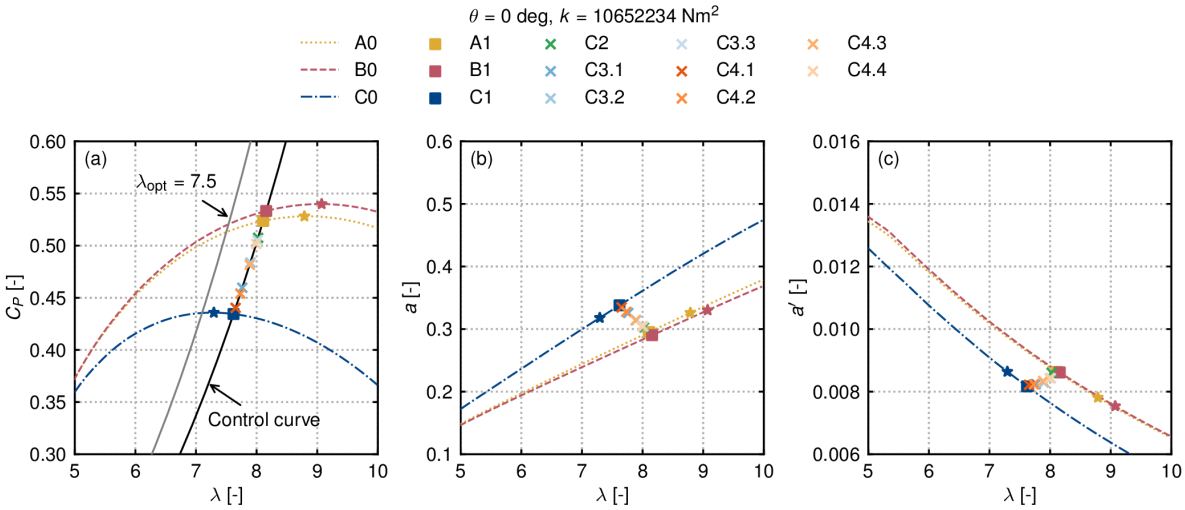

Figure 1: Simulation results for a controller with control constants based on Bak et al. (2013).

constant via an additional simulation that determines C_P at the given tip-speed ratio. We decided to go for the first option as it seems to be the more natural step. When coupling CFD simulations with aeroelastic solvers, the controller in the aeroelastic solver is rarely retuned. In Fig. 1, we also show what the control curve would look like if we had tuned our controller based on an optimal tip-speed ratio of 7.5 for flat terrain as reported by Bak et al. (2013). In this case, the difference to maximum performance in flat terrain would be even more significant, and still, we do not meet maximum performance on top of the hill, because we still do not include the C_P-TSR curve there in our controller tuning.

Overall, it can be seen that our reported differences in performance and the non-optimal operation are not due to our calibration, but rather to the physics constraining the maximum achievable performance and to the k-ω^2 controller being tuneable only to a single optimum in its standard configuration.

Line 218 I'm missing some important discussion points in this section.. It should also include: 1) the role of this specific controller wrt other possible controllers, as mentioned earlier 2) The role of your (lack of) calibration. Unlike what researchers like to believe, wind turbine operators are not idiots. I can't confirm with 100 % certainty, but I think it's safe to assume that operators calibrate each turbine to operate at its optimal CP when it's taken into operation. By simply changing the optimal TSR based, the turbine could likely operate at (close to) its optimum without updating the control law.

We never assumed anything about how operators calibrate turbine controllers, and at this point, we clearly reject any insinuations. We do not consider operators to be "idiots," nor do we see how such a claim could be inferred from the manuscript. We have shown in the introduction that in several research papers, it is not clear whether the utilized controller was tuned for complex terrain/off-design operation conditions, which makes it difficult to interpret performance results, and which motivated this study.

Regarding the other points: 1) including other controllers here would be mostly speculation from our side and we do not want to draw wrong conclusions. Therefore, we do not include them here. For a future study, it is certainly relevant to compare different controllers. 2) Yes, a simple retuning would fix the suboptimal performance. This is addressed in the revised manuscript in l. 286 ff.

Figure 5 What is the value of showing these plots over the radial position mu? From these figures, I would conclude that a is very different for different turbine locations, while a' and alpha are very similar. However, that does not seem to be related to the radial position.

The drawn conclusions that only a is affected by the location when using a torque controller is the intention of this figure. Since a' and specifically α are rather local quantities which depend on the radial position, a plot over the radial position showing their behavior in the different setups seems to be most appropriate from our side. Only claiming they are independent of the position in the text or writing out values for specific positions might not be as convincing. The slightly different results close to the blade root for a' also indicate that our theoretical reasoning in Appendix A is limited to regions of the blade

where drag is negligible.

Line 296 Sure. Or, just calibrate k for an individual turbine location once when putting it in operation, which would likely accomplish a very similar result at much lower complexity
Yes only recalibrating might be an easier solution. However, we explicitly speculate here on why such a recalibration might be difficult due to the small gradients of the quantities of interest. Further, one could speculate that when flow patterns (due to stability and surface coverage) and wind directions change, another recalibration might be possible. An automated algorithm might be beneficial for such scenarios. But at this point we can only speculate and as stated before do not know what is done in practice.

Line 320 The results of these simulations are not shown anywhere else in the paper. You should include these results in your "Results" section before discussing them in your "Discussion" section.
We have included the results of these simulations now also in the results section.

Line 334 f. And how much would that be if better (or any kind of) calibration is performed first?
As we have shown before specifically for the case C0/C1, if we would retune the controller (including adjusting pitch) on top of the hill to maximum performance, the difference to our original tuning would be 2.3 % (20.6 %, losses with controller relative to flat terrain, - 18.3 %, difference between maximum on top of hill and flat terrain). For all other cases, we would also need to simulate the C_P-λ-θ surfaces for a proper retuning, which is computationally expensive. Therefore, we did not do this. However, we expect a similar range of values for these cases.

Line 353 I agree with the limitations discussed here, but I would argue the study has many other limitations too. Just to name a few: 1) simplifying the turbine as and actuator disk 2) Running just one simple type of "baseline" controller 3) The fact that the wind is always flowing perpendicular to the hill
We have added these aspects to the limitations section.

Line 364 a non-calibrated torque-based controller
We have modified the respective sentence (l. 484 in revised manuscript).

Line 366 f. This is a disappointing conclusion, as this was exactly what I had hoped to learn from this paper
In order to improve the expectations for the article, we have adjusted the title so that it reflects the scope of this article more accurately.

Reviewer 2

Review of 'Wind turbine performance and control in complex terrain.'

This article addresses an important topic on optimal control of wind turbines in complex terrain. The authors perform RANS simulations with turbine control to investigate the effect of flow field acceleration on rotor aerodynamic performance. The subject is of interest to the wind energy community. However, there are several aspects that need to be addressed before the article can be published.

1. The results appear to be very terrain-specific. What general lessons can one draw from the study apart from the fact that turbine control is terrain dependent?
   Indeed, the results are highly terrain-dependent. However, this study allows for several more general conclusions. First, it yields insight on how exactly a k-ω^2 controller operates in off-design conditions, keeping rotor quantities instead of free-stream quantities constant (Sect. 4.1.1). Further, it is shown, that this controller maintains constant tangential induction and angles of attack (Sect. 4.2.2). Last, it is shown that the usage of speed-up factors in site assessment likely yields overprediction of expected performance (Sect. 4.3).

2. How are the turbine positions chosen? I understand that it is natural to place a turbine at the hilltop, but why at the foot of the hill? If the wind speed changes by 180°, the turbine placed at the foot of the hill will be in its wake. What happens then? I think the choice of turbine locations should be justified.
   The location at the foot of the hill is motivated by the intention to not only analyze a situation in

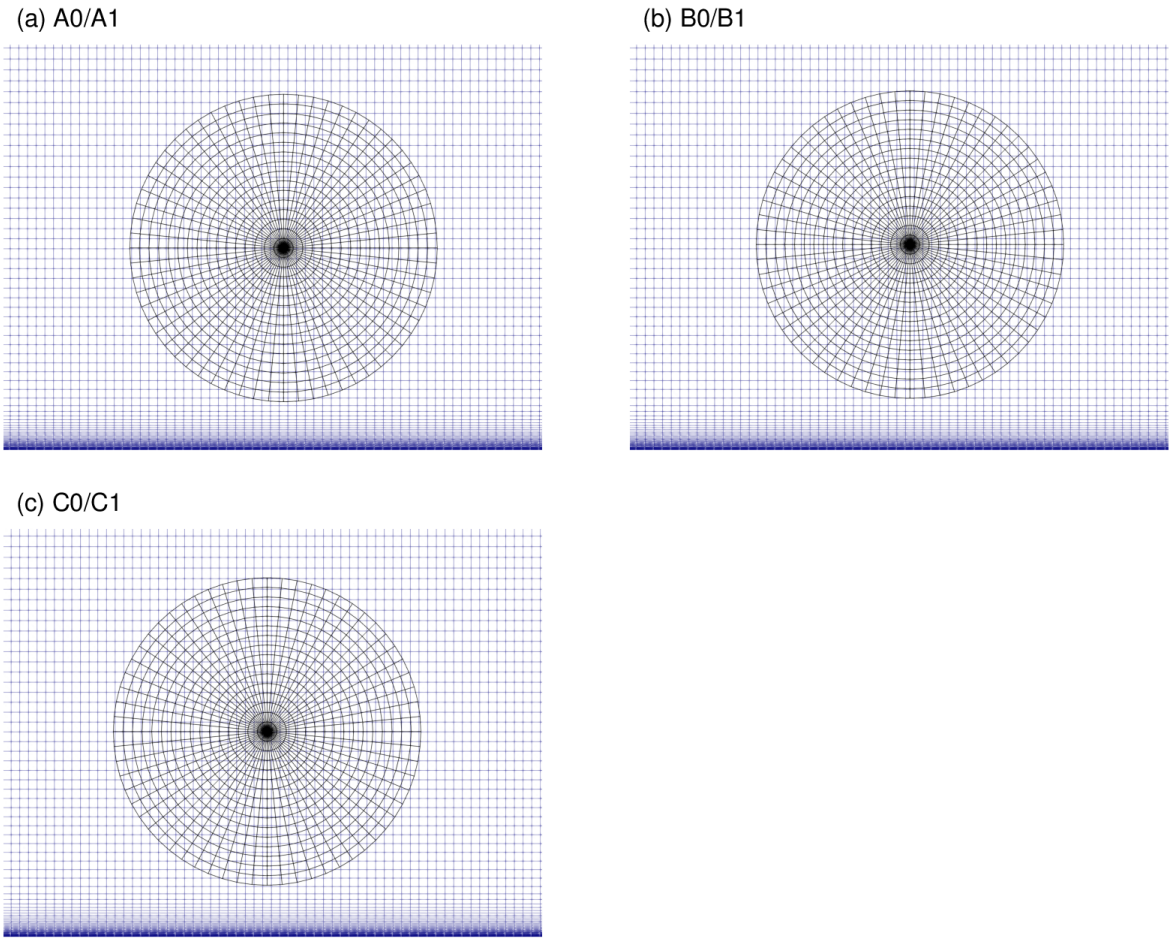

Figure 2: Close-up of the computational grids in the actuator disk region in the y-z plane for **(a)** the flat terrain simulations, **(b)** the simulations of a turbine ahead of the hill, and **(c)** the simulations of the turbine on the hill.

which a wind turbine underperforms, but also a situation in which it overperforms relative to flat terrain. At the foot of the hill, the flow accelerates, leading to the desired overperformance. We admit that this location is unlikely to be chosen in practice because, as stated, when the wind direction changes, the inflow will change significantly, likely leading to lower performance. Thus, it is rather an academic case that solidifies the conclusions drawn in this work. We have added an explanation also to the manuscript (l. 88 f.).

3. While discussing Figure 3(a), the authors mention that the turbine at the foot of the hill produces 'slightly more' power than that in flat terrain. However, visually, I cannot see any difference between the two curves. If indeed there is a very small improvement, is it higher than any uncertainty in the quantification of power from simulations?
   The difference in power mentioned in the context of Fig. 3 (a) of the original manuscript is more clearly visible in Fig. 3 (b) of the original manuscript or Fig. 6 (a) of the revised manuscript, where the power coefficient is visualized. Besides the grid-refinement study, we have not conducted an uncertainty assessment. However, in all cases, the computational grids in the actuator disk region are very similar, as seen in Fig. 2. We would therefore argue that any error in the power quantification is a systematic error that should exist to a similar extent in all results and therefore cancels out when performing relative comparisons. This argument is supported by Fig. 3 showing the relative change of the ratio of reference wind speed ahead or on top of the hill to the one in flat terrain in (a) and the respective ratios of power coefficients in (b) when varying the cell size.

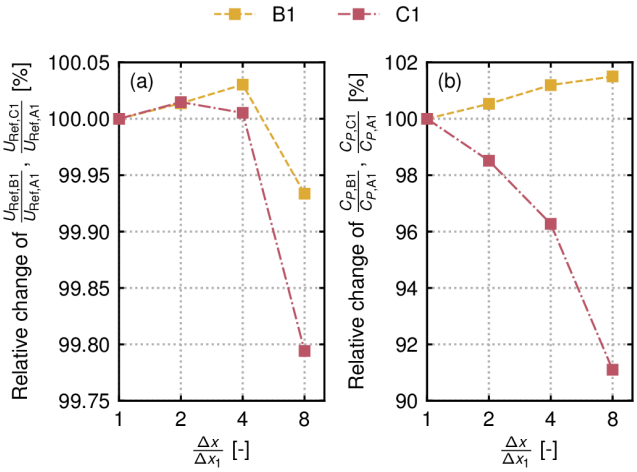

Figure 3: Relative change of the ratio between reference wind speeds ahead of the hill or on top of the hill and the wind speed in flat terrain for varying the cell size in **(a)** and respective relative change in power coefficient in **(b)**. Note that the results for the power coefficient include the controller.

By increasing the cell side length by a factor of two, the reference wind speed ratio changes by less than 0.02 %. The power coefficient ratio varies in this case by around 0.5 % ahead of the hill and by 1.5 % on top of it. It is important to keep in mind here that the simulations also include a controller, which is an additional source of uncertainty. Only the reference wind speed, which is evaluated on the actuator disk grid, is obtained without a controller. Therefore, the reference wind speed shows the actual grid dependency of our method without additional uncertainty sources due to the controller. A simulation without a controller, where for a fixed rotor speed and pitch, the power is evaluated, likely has a similar convergence behavior as the reference wind speed evaluation. Fig. 6 in the revised manuscript further shows that the C_P-λ curve ahead of the hill, obtained without a controller, also exhibits higher performance. The simulation with the controller settles on this curve.

4. The authors discuss in detail what leads to the sub-optimal performance of turbines on a hill. However, they do not demonstrate any control strategy that could lead to a better turbine performance in a non-uniform background flow.
   We deliberately decided not to develop a control strategy to improve turbine performance in non-uniform background flow. It is, in our view, outside the scope of this work, which aims to improve understanding of a control paradigm widely used in research (generator torque control in region 2 of the power curve). The work was motivated by the question of how performance results in complex terrain need to be interpreted with respect to the chosen control algorithm, which is addressed here for steady-state simulations. While it would indeed be of interest how one can optimize power capture in such scenarios (control algorithms which seek optimal power performance already exist, see e.g. Creaby et al. (2009)), we believe there is more value in performing such an analysis in a transient environment and therefore leave this question to a future investigation. In the manuscript, we also argue that a simple re-tuning of the control constants would yield a better performance.

5. There are many grammatical and typographical errors, especially in the abstract and introduction. In general, the writing quality can be improved.
   We carefully proofread the entire article with emphasis on the abstract and introduction, and corrected potential grammatical and typographical errors. If the quality is insufficient, we kindly ask for specific points that need to be corrected and or improved.

References

Christian Bak, Frederik Zahle, Robert Bitsche, Taeseong Klm, Anders Yde, Lars Christian Henriksen, Anand Natarajan, and Morten Hartvig Hansen. Description of the DTU 10 MW Reference Wind Turbine. Technical Report DTU Wind Energy Report-I-0092, DTU Wind Energy, Roskilde, Denmark, 2013.

Fernando D. Bianchi, Ricardo J. Mantz, and Hernán de Battista. *Wind Turbine Control Systems: Principles, Modelling and Gain Scheduling Design*. Advances in Industrial Control. Springer London, London, 2007. ISBN 978-1-84628-492-2.

Justin Creaby, Yaoyu Li, and John E. Seem. Maximizing Wind Turbine Energy Capture Using Multivariable Extremum Seeking Control. *Wind Engineering*, 33(4):361–387, 2009. doi: 10.1260/030952409789685753.

E L Hodgson, S J Andersen, N Troldborg, A Meyer Forsting, R F Mikkelsen, and J N Sørensen. A Quantitative Comparison of Aeroelastic Computations using Flex5 and Actuator Methods in LES. *Journal of Physics: Conference Series*, 1934(1):012014, 2021. doi: 10.1088/1742-6596/1934/1/012014.

K E Johnson, L Y Pao, M J Balas, and L J Fingerish. Control of variable-speed wind turbines: standard and adaptive techniques for maximizing energy capture. *IEEE Control Systems*, 26(3):70–81, 2006. doi: 10.1109/mcs.2006.1636311.

Luoqin Liu and Richard J. A. M. Stevens. Effects of Two-Dimensional Steep Hills on the Performance of Wind Turbines and Wind Farms. *Boundary-Layer Meteorology*, 176(2):251–269, 2020. doi: 10.5194/wes-7-1527-2022.

Alok Mishra, Nitish Arya, and Amitabh Bhattacharya. Wake steering of wind turbine in the presence of a two-dimensional hill. *Physics of Fluids*, 36(4):045125, 2024. doi: 10.1063/5.0185842.

Niels Troldborg, Søren J. Andersen, Emily L. Hodgson, and Alexander Meyer Forsting. Brief communication: How does complex terrain change the power curve of a wind turbine? *Wind Energy Science*, 7(4):1527–1532, 2022. doi: 10.5194/wes-7-1527-2022.

C P Zengler, N Troldborg, and M Gaunaa. Is the free wind speed sufficient to determine aerodynamic turbine performance in complex terrain? *Journal of Physics: Conference Series*, 2767(9):092049, 2024. doi: 10.1088/1742-6596/2767/9/092049.

Clemens Paul Zengler, Niels Troldborg, and Mac Gaunaa. Modeling the influence of streamwise flow field acceleration on the aerodynamic performance of an actuator disk. *Wind Energy Science*, 10(7): 1485–1497, 2025. doi: 10.5194/wes-10-1485-2025.

Stig Øye. Flex4 simulation of wind turbine dynamics. In *Proc. of 28th IEA Meeting of Experts Concerning State of the Art of Aeroelastic Codes for Wind Turbine Calculations*, pages 71–76, Lyngby, Denmark, 1996. IEA.

Aerodynamic analysis of standard variable-speed torque control in complex terrain

Clemens Paul Zengler[1], Mac Gaunaa[1], and Niels Troldborg[1]

[1]Department of Wind and Energy Systems, Technical University of Denmark. Frederiksborgvej 399, 4000 Roskilde, Denmark

Correspondence: Clemens Paul Zengler (clezen@dtu.dk)

Abstract. Wind energy projects in complex terrain are often associated with high uncertainties regarding the expected power performance. These uncertainties are mostly attributed to difficulties in obtaining reliable wind speed estimates. ~~However, an additional factor is~~ Two additional factors are that the physical limits of energy extraction vary in these cases, and that the employed wind turbine might operate differently than expected in these conditions. This study addresses these two factors with the goals of identifying the dominant factor influencing power performance and improving understanding of how a turbine controller operates in flow conditions for which it was not calibrated. For this purpose, Reynolds-averaged Navier-Stokes (RANS) simulations of a wind turbine modeled as an actuator disk (AD) subject to a neutral atmospheric inflow are performed. The influence of the turbine position relative to a quasi-two-dimensional Gaussian hill on the maximum power performance and on the response of a torque controller in region ~~two~~ 2 of the power curve is investigated. ~~When~~ It is found that when the turbine is located at the foot of the hill, the maximum power coefficient increases by ~~3.5%. At the top of the hill, the maximum power decreases by 20.0% . A consequenceof this is that~~2.46 %, while it decreases by 18.25 % on top of the hill. As a consequence, when placing wind turbines on elevated locations, the power does not scale with the cube of the increase ~~of~~ in wind speed. ~~It is furthermore found, that the torque controller operates in a way, that local flow angles remain constant~~ The controller maintains a constant local power coefficient, i.e., ~~irrespectively of the location of the turbine. Also,~~ the power coefficient based on the disturbed ~~wind speed in the rotorplane remains constant, which~~ rotor-plane velocity. This local power coefficient does not necessarily coincide with the ~~maximum power coefficient based on~~ optimal power coefficient defined using the undisturbed wind speed. As a ~~consequence, a torque~~ result, the controller does not track ~~maximum performance~~ optimal performance when the relationship between undisturbed and disturbed wind speed differs from the calibration conditions, such as when a controller tuned for flat terrain is applied in complex terrain. In the present study, this mismatch leads to a maximum power loss of 1.96 %. Overall, this study sheds light on the interpretation of ~~performance results of wind turbines~~ wind turbine performance results in complex terrain and helps ~~to~~ shape efforts to ~~decrease~~ reduce prediction uncertainties for future onshore wind projects in complex terrain.

1 Introduction

~~An example of a power curve of a wind turbine with the different control regions labeled: (a) Power and (b) rotor speed ω and blade pitch θ.Wind turbine control~~ Wind turbine operation can be roughly divided into three regions depending on the

undisturbed wind speed. In region ~~one~~1, no power is extracted, in region ~~two~~2, the primary objective is to maximize ~~energy extraction from the flow field~~power performance, and in region ~~three~~3, the power generation is kept constant. ~~An example of a power curve with these three regions and the respective rotor speed and~~ Generally, the generator torque and the collective blade pitch ~~is presented in Fig. ??. Also, regions 1.5 and 2.5 are shown, which are commonly used to set a minimum rotor speed and~~ are used to ~~reduce loads and noise (Abbas et al., 2022). In this work, we focus solely on analyzing region two from an aerodynamic perspective, where it is traditionally attempted to maintain a constant power and thrust coefficient to primarily extract as much energy as possible from the flow. Nonetheless, for the sake of completeness, the other regions are included in the simulations as well.~~ control the turbine (Abbas et al., 2022), and since the undisturbed wind speed can be difficult to evaluate, the generator speed often serves as a control input. Control tuning is usually based on aeroelastic simulations of the turbine of interest, as has been done, for example, for the NREL 5 MW reference wind turbine (RWT) (Jonkman et al., 2009) or the DTU 10 MW RWT (Bak et al., 2013).

In region 2, constraints on performance optimization often stem from load considerations, where optimum performance is sacrificed for a reduction in loads. However, this work is only concerned about maximum performance in region 2 and hence does not consider loads.

~~But what is actually the available energy in the flow? Recent~~ During the identification of the points of maximum performance in aeroelastic simulations, the mean flow is usually assumed to vary over the rotor area due to vertical shear and yaw misalignment, but is assumed uniform in the streamwise direction. These conditions are fulfilled in flat terrain but not in complex terrain, where topography induces significant streamwise flow variations, due to hills, elevations, ramps, and other features. An analysis of a simplified analytical model capturing the effects of acceleration induced by complex terrain has shown that, in such conditions, the maximum performance and the point of optimal operation of a constantly loaded actuator disk (AD) change (Zengler et al., 2025a). This raises the question of whether a controller tuned in flat terrain conditions still tracks optimal performance in region 2 when operating in complex terrain.

In general, recent research has shown that using only local ~~hub position quantities, like the free wind speed~~ rotor quantities, such as the undisturbed wind speed at the turbine position, is insufficient to quantify ~~this energycontent~~the extractable energy, but also the streamwise development of the ~~free wind speed needs to~~ undisturbed wind speed must be taken into account (Troldborg et al., 2022; Zengler et al., 2024; Revaz and Porté-Agel, 2024). In other words, ~~the location of a wind turbineand the~~ both the turbine's location and the local development of the flow ~~around this location~~ field affect the power performance quantified by the power coefficient. A streamwise acceleration of the flow leads to an increase of ~~power~~the power coefficient, while a deceleration leads to a decrease (Dar et al., 2023). ~~On the one side, power performance models that consider this effect are solely~~ Besides the simple model mentioned above, several other models based on conservation equations ~~(Cai et al., 2021; Zengler et al., 2025a; Dar et al., 2025) without considering the controller. And on the other side, studies on~~ have been developed to describe this effect (Cai et al., 2021; Dar et al., 2025, 2026).

Studies on wind turbine performance in complex terrain often rely on ~~certain controllers (Revaz and Porté-Agel, 2024; Liu and Stevens, 2~~ specific controllers without actively investigating the influence of the ~~control choice on performanceresults. This makes it difficult to draw definite conclusions from these studies, because the exact interaction between controller and~~ chosen

controller and its tuning on performance. In a large-eddy simulation (LES) study investigating the influence of a hill on the power performance of individual turbines and wind farms, Liu and Stevens (2020) scale the rotor forces based on the disturbed disk-averaged velocity and a prescribed modified thrust coefficient based on the disturbed disk-averaged velocity as proposed by Meyers and Meneveau (2010). This thrust coefficient is determined in advance and does not appear to be tuned to maximize power extraction in the investigated cases. Revaz and Porté-Agel (2024) and Dar et al. (2025) do not explicitly state the controller used in their LES-studies of wind turbines in streamwise non-uniform ~~background flow is not clear.~~

~~A common way of controlling a wind turbine in region two of the power curve uses a torque controller, which sets the generator torque to enforce the appropriate equilibrium between generator and rotor torque (Bossanyi, 2000; Pao and Johnson, 2011) . It relies on the rotational speed of the rotor as input, which, unlike wind speed, can be easily measured in both real life and simulation environments. To derive the torque control law, we start with the power which can be calculated for a given wind speed U_{Ref} as~~

~~$$P = \frac{1}{2}\rho R^2 \pi C_P(\lambda, \theta, X)\, U_{\mathrm{Ref}}^3,$$~~

~~with air density ρ, rotor radius R, and power coefficient C_P which depends on the~~ flows, but it seems to be the one described by Wu and Porté-Agel (2015), which sets the rotor speed based on a prescribed relation between torque and rotor speed in an iterative procedure. In both studies, the tip-speed ratio ~~$\lambda = \omega R / U_{\mathrm{Ref}}$, the blade pitch θ, and also on the location X, as the aforementioned research shows. In the following, these dependencies will not be explicitly mentioned. The rotor torque is related to the power as~~

~~$$\tau = \frac{P}{\omega} = \frac{1}{2}\rho R^2 \pi C_P \frac{U_{\mathrm{Ref}}^3}{\omega},$$~~

~~In order to design a torque controller , it is desired to keep the local flow angles at the blade constant at the conditions, where maximum $C_{P,\mathrm{max}}$ is reached. This means that~~ necessary to evaluate the turbine's operational state, is not reported. Mishra et al. (2024) use the reference open-source controller ROSCO developed by Abbas et al. (2022) for their study of a wind turbine ahead of a quasi-two-dimensional hill without stating which of the two control strategies available in the ~~tip-speed ratio must remain constant. By substituting $U_{\mathrm{Ref}} = \omega R / \lambda_{\mathrm{opt}}$, one obtains (Bossanyi, 2000; Bianchi et al., 2007)~~

~~$$\tau = \underbrace{\frac{1}{2}\rho R^5 \pi \frac{C_{P,\mathrm{max}}}{\lambda_{\mathrm{opt}}^3}}_{k} \omega^2 = k\omega^2,$$~~

~~where the torque constant k is introduced. This equation can now be used to set the generator torque τ_{Gen} as a function of the rotor speed to ensure optimal operation. As the name suggests, k is kept constant in this case, representing optimal operation in the environment the controller was calibrated for . The substitution of U_{Ref} in order to maintain constant local flow angles is essential to understand how a torque controller works from an aerodynamic perspective. Of course, the controller does not track the local flow angles. But maintaining $\tau \propto \omega^2$ is from an aerodynamic perspective only possible when aerodynamic forces also scale with the rotor speed squared, which is only the case, when local flow angles are kept constant This will become apparent~~

~~in the course of this paper. For now, we will adhere to the traditional approach of evaluating wind turbine performance in terms of power coefficient and tip-speed ratio. In steady state, conservation of angular momentum between the rotor and the generator yields~~

$$\tau_{\mathrm{Gen}} = \tau_{\mathrm{Aero}} \Leftrightarrow k\omega^2 = \frac{1}{2}\rho R^5 \pi \frac{C_P}{\lambda^3}\omega^2 \Leftrightarrow \frac{C_{P,\max}}{\lambda_{\mathrm{opt}}^3} = \frac{C_P}{\lambda^3}.$$

~~This means that for our example of a turbine in flat terrain, the turbine will always track the curve defined by $\frac{C_{P,\max}}{\lambda_{\mathrm{opt}}^3} = \frac{C_P}{\lambda^3}$.~~ controller for region 2 is used. Prospathopoulos et al. (2010) performed Reynolds-averaged Navier-Stokes (RANS) simulations of an existing wind farm in complex terrain and compared three different ways of controlling the thrust coefficient in terms of how well they match the measured power. They set the thrust coefficient either on the basis of the wind speed one diameter upstream of the turbine, from an induction-based estimate, or sequentially by evaluating the undisturbed wind speed when the respective turbine is switched off. The last method showed the best agreement with measurements, but the reasons for this were not evaluated in detail. Overall, these studies show a literature gap regarding how exactly the control choice affects reported power performance. This makes it difficult to draw definite conclusions about performance from these studies, as it is unclear whether the controller continues to maintain its primary control objective of tracking optimal performance in complex terrain.

~~In computational fluid dynamics (CFD), an alternative to this type of control is to set the rotor speed (and also the blade pitch) directly~~ A common way of controlling a wind turbine in region 2 of the power curve sets the generator torque τ_{Gen} as a function of the ~~wind speed in the rotor plane during operation of the turbine based on a calibration procedure carried out in advance (van der Laan et al., 2014). It was previously shown that this approach is equivalent to a torque controller in region two because in this region, rotational speed and disk velocity are linked by a constant (Zengler et al., 2025b).~~ generator speed ω according to $\tau_{\mathrm{Gen}} = k\omega^2$, enforcing an equilibrium between generator and rotor torque in steady state (Bossanyi, 2000; Pao and Johnson, 2011; Johnson et al., 2006). This strategy is referred to as k-ω^2 control and implemented in many turbine controllers and aeroelastic simulation tools, such as ROSCO (Abbas et al., 2022), OpenFAST (Jonkman et al., 2026), Flex5 (Øye, 1996), and HAWC2 (Larsen and Hansen, 2025; Hansen and Henriksen, 2013). The torque constant k can be set based on the optimal power coefficient and tip-speed ratio, which are determined in advance through aeroelastic simulations in flat terrain conditions as mentioned before.

~~The derivation of the torque control law indicates that the power coefficient is an essential part of the control design. However, it also depends on the background flow, raising the question of what impact~~ In a previous work, the analytical model describing the effect of streamwise acceleration on the induction of a uniformly loaded AD (Zengler et al., 2025a) was implemented into a blade-element-momentum model and coupled with a k-ω^2 controller. The study showed that, in an accelerating flow, a controller tuned ~~to flat terrain has on the performance of the turbine located~~ for uniform inflow does not achieve optimal performance (Zengler et al., 2025b). The present study aims to confirm this result in a more realistic setting by performing steady-state RANS simulations of an AD in complex terrain ~~. This study seeks to entangle controller and complex terrain effects and therefore contribute to a deeper understanding of simulation results and turbine operation~~ with resolved blade loads. Thus, the analytical flow model representing the acceleration in Zengler et al. (2025b) is replaced by the RANS equations. This allows for more robust conclusions and also addresses quantities such as axial and tangential induction, which have not yet been

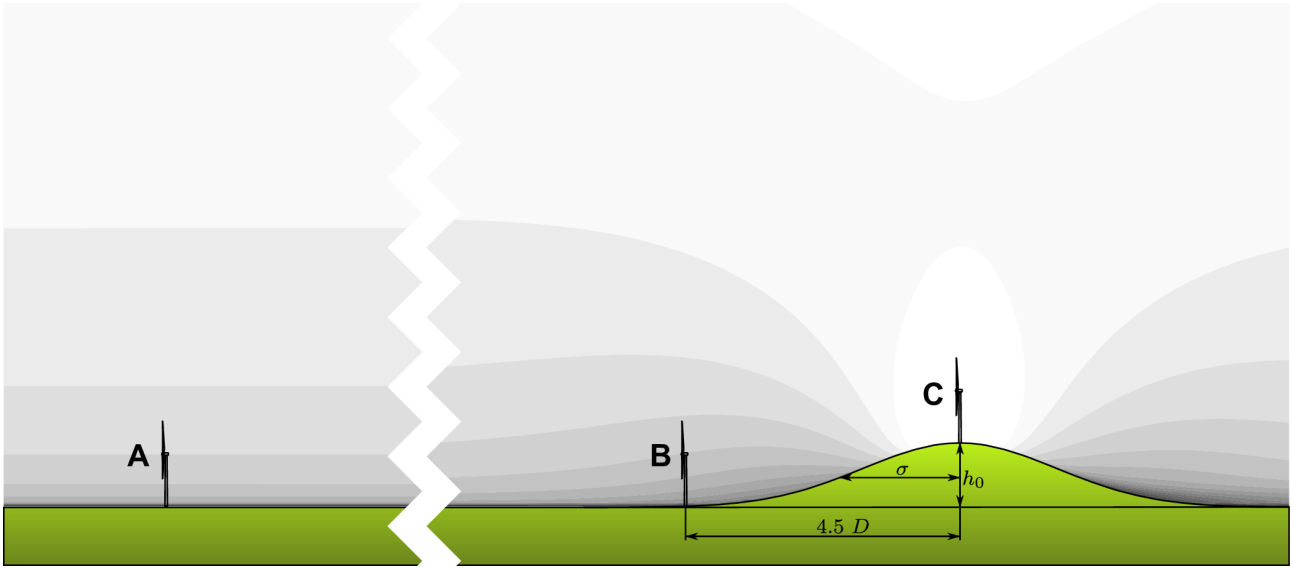

Figure 1. Sketch of the terrain setup with the three considered turbine locations.

analyzed in the context of control in complex terrain. ~~For this purpose, the steady-state control of a wind turbine in streamwise non-uniform flow fields is investigated through CFD simulations of an actuator disk (AD) located at different positions relative to a hill, and the results are discussed based on theoretical considerations. To the knowledge of the authors, this work for the first time investigates the influence of streamwise non-uniformity of the flow field on wind turbine control.~~ In addition, the impact of non-constant power coefficients in complex terrain on the usage of speed-up factors is investigated, yielding a deeper understanding of the expected power increase by placing turbines on elevated position.

The work is structured as follows: ~~Sec.~~ Section 2 presents the methodology~~which is largely based on previous works, Sec~~, Sect. 3 presents the results~~and Sec. 4 .~~, and Sect. 4 discusses the results and ~~put~~ puts them in a broader context. The work concludes in Sect. 5. In appendix A and B, supporting analytical considerations regarding tangential induction and maximum power performance are provided.

2 Methodology

Simulations of a turbine in three different terrain setups are considered, as shown in Fig. 41. In the first case (**A**), the turbine is operating in flat terrain, with no obstacles present. In the second case (**B**), the turbine is located at the foot of a hill, which accelerates the wake flow. The hill ~~itself~~ is quasi-two-dimensional, parametrized by a Gaussian function ~~.~~as defined in Sect. 2.4. The direction of the onset wind is perpendicular to the ridge of the hill, resulting in a quasi-two-dimensional flow field when the turbine is not operating. In the last case (**C**), the turbine is located on the ridge of the hill, which results in a deceleration of the wake. ~~For the last case~~Locations **B** and **C** are chosen because they would result in an increase or decrease of

performance relative to location **A**, respectively, which allows for drawing conclusions for both accelerating and decelerating cases. For location **C**, additional simulations with varying hill height, width, and surface roughness are performed. ~~These are not analyzed in detail but serve as support for arguments made in the discussion presented in Sec. 4. The direction of the onset wind is perpendicular to the ridge of the hill, resulting in a quasi-two-dimensional flow field when the turbine is not operating. In general, the~~ The flow setup is similar to ~~the one described by Zengler et al. (2024), employing Reynolds-averaged Navier-Stokes (RANS) simulations of a~~ a previous work (Zengler et al., 2024), employing RANS simulations of an AD on a quasi-two-dimensional Gaussian hill subject to a neutral atmospheric inflow.

2.1 Turbine model

The blade geometries of the DTU 10 MW RWT with a rotor diameter of 178.3 m and a hub height of 119 m are used ~~for the simulations (Bak et al., 2013).~~ (Bak et al., 2013). Tower, nacelle, and hub are not included in the simulation.

2.2 ~~Controller~~k-ω^2 control

~~A traditional pitch-torque control algorithm as described by Jonkman et al. (2009) is used to control the rotational speed of the turbine. As mentioned before, the generator torque in region two is calculated as~~ The turbine is controlled by the k-ω^2 controller in region 2 of the power curve. It relies on the generator's rotational speed, ω, as input. For simplicity, we assume the turbine is a direct-drive turbine, meaning the generator and rotor speeds are equal when losses are neglected. In order to understand the underlying assumptions of k-ω^2 control, the control law will be derived in the following. We start with the turbine power, which for a given wind speed U_{Ref} can be calculated as

$$P = \frac{1}{2}\rho R^2 \pi C_P(\lambda, \theta, X)\, U_{\mathrm{Ref}}^3, \tag{1}$$

with air density ρ, rotor radius R, and power coefficient C_P which depends on the tip-speed ratio $\lambda = \omega R / U_{\mathrm{Ref}}$, the blade pitch θ, and also on the location X, as the aforementioned research shows (Troldborg et al., 2022; Zengler et al., 2024; Revaz and Porté-Agel, 20 . In the following, these dependencies will not be explicitly mentioned. The definition of the reference wind speed U_{Ref} will be provided in Sect. 2.3. The rotor torque is related to the power as

$$\tau_{\mathrm{GenRot}} = k\omega \frac{P}{\omega} = \frac{1}{2}\rho R^2 \pi C_P \frac{U_{\mathrm{Ref}}^3}{\omega}. \tag{2}$$

~~where the~~ To design a controller that tracks optimal performance, it is desired to keep the local inflow angles at the blade constant under the conditions where the maximum power coefficient $C_{P\max}$ is reached. This means that the tip-speed ratio must remain constant at optimal conditions. By substituting $U_{\mathrm{Ref}} = \omega R / \lambda_{\mathrm{opt}}$, one obtains (Bossanyi, 2000; Bianchi et al., 2007)

$$\tau_{\mathrm{Rot,\,opt}} = \underbrace{\frac{1}{2}\rho R^5 \pi \frac{C_{P\max}}{\lambda_{\mathrm{opt}}^3}}_{k} \omega^2, \tag{3}$$

where the torque constant k is introduced, representing optimal operational conditions in the given environment. This equation can now be used to set the generator torque τ_{Gen} as a function of the rotor speed to ensure optimal operation

$$k\tau_{\mathrm{Gen}} = \frac{1}{2}\rho\pi R^5 \frac{C_{P,\max}}{\lambda_{\mathrm{opt}}^3} k\omega^2. \tag{4}$$

The ~~values of $C_{P,\max}$ and λ_{opt} are obtained from the simulated flat terrain C_P~~substitution of U_{Ref} to maintain constant local inflow angles at the blade is essential for understanding how the controller works from an aerodynamic perspective. Of course, the controller does not measure the inflow angles. But maintaining $\tau_{\mathrm{Rot}} \propto \omega^2$ is, from an aerodynamic perspective, only possible when aerodynamic forces also scale with the rotor speed squared, which is only the case when local inflow angles at the blades are kept constant. This will become apparent in the course of this paper. In steady state, conservation of angular momentum between the rotor and the generator yields

$$\tau_{\mathrm{Gen}} = \tau_{\mathrm{Rot}} \tag{5}$$

$$\Leftrightarrow k\omega^2 = \frac{1}{2}\rho R^5 \pi \frac{C_P}{\lambda^3}\omega^2 \tag{6}$$

$$\Leftrightarrow \frac{C_{P\max}}{\lambda_{\mathrm{opt}}^3} = \frac{C_P}{\lambda^3}, \tag{7}$$

Thus, the turbine will always track the curve defined by Eq. (7), irrespective of the surrounding flow.

In this work, the k-~~λ-pitch surface later presented in Fig. 4 at the blade pitch θ_{opt} which maximizes the power coefficient. In~~ ω^2 controller is implemented as part of a 5-region generator torque controller as described by Jonkman et al. (2009). In every iteration i of the simulation, ω is updated until convergence based on the conservation of angular momentum of the rotor~~as~~, which can be written as

$$\omega_{i+1} = \omega_i + \frac{\Delta t}{J}\left(\tau_{\mathrm{Aero},i\mathrm{Rot},i} - \tau_{\mathrm{Gen},i}\right), \tag{8}$$

with the ~~pseudo-time~~ time step Δt, the rotor moment of inertia J and the ~~aerodynamic torque $\tau_{\mathrm{Aero},i}$~~rotor torque $\tau_{\mathrm{Rot},i}$, which is extracted from the flow simulation. A low-pass filter for the rotational speed is used in Eq. (8)~~as described by Jonkman et al. (2009). In a~~. In steady state, aerodynamic torque and generator torque ~~need to be in balance, which ensures that below rated wind speed in flat terrain~~are balanced, ensuring that in region 2, the turbine tracks maximum power performance ~~. Because~~ in flat terrain. Since steady-state simulations are performed, the dynamic response of the controller is not of interest here, and $\Delta t/J$ in Eq. (8) is solely tuned to improve solution convergence. ~~Above rated wind speed,~~ The blade pitch is controlled by a proportional-integral (PI) controller ~~modifies the pitch to maintain the~~ as also described by Jonkman et al. (2009), which modifies the blade pitch above rated conditions to maintain rated rotor speed and consequently power. By design, the PI controller saturates below rated conditions at θ_{opt}.

The optimal blade pitch θ_{opt}, tip-speed ratio λ_{opt} and power coefficient $C_{P\max}$ can be obtained from aeroelastic simulations of the turbine without the flow field being resolved by CFD as it has also been done for the DTU 10 MW RWT by Bak et al. (2013)

Table 1. Controller settings investigated within this study. Note that the torque constant for the default control settings from Bak et al. (2013) is adjusted for the generator efficiency of 0.94.

Case	θ_{opt} [deg]	k [Nms^2]
Bak et al. (2013)	0.0	10652234
This work	-1.94	11169578

. The optimum identified in this way is not necessarily the same optimum as it can be found when resolving the flow field with CFD. In this work, we chose to tune the control constants based on our RANS simulation setup, as shown later in Sect. 3.2. The resulting control constants are listed in Table 1.

2.3 Reference wind speed and normalization of quantities

We introduce the following decomposition of the mean flow:

$$u = U + u', \tag{9}$$

where u is the flow field including the turbine interacting with it, U is the undisturbed flow field, and u' quantifies the disturbance by the turbine. The reference wind speed employed throughout this work is the undisturbed rotor-equivalent wind speed~~(Wagner et al., 2011) calculated as~~ , which we calculated not only as an average over height as originally proposed by Wagner et al. (2011), but over the lateral dimension as well as

$$U_{\mathrm{Ref}} = \sqrt[3]{\frac{1}{A_{\mathrm{R}}}\frac{1}{A_R}\int_{A_{\mathrm{R}}}\int_{A_R} U_R^3 dA}, \tag{10}$$

with U_R being the undisturbed rotor-normal velocity component at the location of the rotor. This approach takes the variation of available kinetic energy over the rotor plane into account, and allows for a more accurate assessment of the efficiency of a turbine. However, it does not consider the streamwise development of the undisturbed flow field.

At every turbine location, U_{Ref} is obtained separately~~, thus~~ . Therefore, quantities like λ, C_P, and the axial induction a are normalized by the respective local U_{Ref} evaluated when the turbine is turned off and not by an upstream velocity. By defining the reference wind speed like this, any bias in the performance results due to a change in kinetic energy of the flow induced by the topography between wind speed measurement position and turbine position is avoided. It is also more consistent defining the reference wind speed like this compared to choosing an arbitrary position upstream, where the relation between the wind speed at this position and the turbine position depends on the terrain.

In Sect. 4.3, the case of a turbine placed on top of a hill (location **C**) is used to analyze the combined effect of the increased kinetic energy at the turbine position and the flow deceleration behind the hill.

2.4 Domain and grid design

The shape of the quasi-two-dimensional Gaussian hill is described by

$$h = h_0 \exp\left(-\frac{x^2}{2\sigma^2}\right), \tag{11}$$

and has, in its standard configuration, a height h_0 of 1 ~~D~~ D and a standard width σ of 1.5 ~~D with D~~ D, with D denoting the turbine diameter. When the turbine is located ~~ahead~~/at the foot of the hill (**B**), it is 4.5 ~~D~~ D away from the top of the hill. The surface roughness is 0.001 m, ~~which corresponds~~ corresponding to a snowy surface ~~in reality (Troen and Petersen, 1989) . Three~~ (Troen and Petersen, 1989). Due to this low roughness, the flow does not separate behind the crest, leading to a strong deceleration and noticeable impact on the induction (Zengler et al., 2024). The configuration as a whole is chosen because it modifies the flow in the proximity of the AD at a length scale comparable to the rotor size. When characteristic lengths of the hill, such as height or width, are significantly smaller than the turbine, its impact on performance vanishes, and the same holds when the hill is significantly bigger than the turbine (Revaz and Porté-Agel, 2024). Effectively, the turbine is subject to a flow comparable to flat terrain in such cases. The setup is similar in dimensions to other studies (Liu and Stevens, 2020; Mishra et al., 2024; Trolc but purposely idealized to investigate the isolated effect of flow acceleration and deceleration. To allow for more general conclusions, three additional sets of simulations of the turbine on top of the hill are performed. In ~~one case~~the first set (**C2**), the surface roughness is changed to 0.1 m~~, in the next one~~. In the second set (**C3.X**), the hill height is varied while the width is kept constant, and in the last ~~case, the ratio between~~ set (**C4.X**), both hill height and width ~~is kept constant, while the height is varied.~~ are scaled with the same scaling factor, thus keeping the ratio between height and width constant.

An overview of all simulations is listed in ~~Tab.~~ Table 2. The simulations are performed in two steps: First, the domain is simulated without the turbine to extract the undisturbed U_{Ref} at the turbine position. Second, after convergence of the empty domain, the turbine is ~~switched on~~placed into the domain, and the simulation ~~converged~~ is run until convergence again to extract ~~power, induction, etc~~the relevant turbine and flow metrics.

~~The~~ In all cases, the computational domain is ~~in all cases~~ a curvilinear grid with a size of 45 $\times$ 18 $\times$ 34 ~~D^3~~ D^3 in the x, y and z direction, respectively, which correspond to the streamwise, lateral~~and vertical dimension~~, and vertical dimensions, respectively. The hill is generated by deforming the bottom surface of a flat domain. In total, the grid has a size of 256 $\times$ 192 $\times$ 192 $=$ 9437184 cells. In the turbine region, the mesh is refined with nearly cubic cells with a side length of ~~5 m, corresponding to a resolution of nearly 36 cells per D~~approximately $D/32$.

The turbine is simulated as an ~~actuator disk~~AD, which is represented in the flow domain by a polar grid, and forces are projected onto the computational grid by the actuator shape approach (Réthoré et al., 2014; Troldborg et al., 2015). The tip-loss correction by Glauert is applied and the disk grid has 17 radial points and 64 azimuthal points.

~~For the case with the turbine located on the hill ridge, a sensitivity study the domain size has been performed by Zengler et al. (2024) showing a variation of the disk-averaged velocity for a fixed C_T of less than 0.1 % when increasing the cross-sectional area of the domain by a factor of eight. A sensitivity analysis of the cell size is carried out in this work, showing that U_{Ref} varies by less than 0.01 % when increasing the cell volume by a factor of eight. When the turbine is operating with a controller, the induction and power between these two different cell volumes vary by less than 2 %.~~

Table 2. Conducted simulations within this study. The controller is tuned based on optimal operation obtained from **A0**.

Label	Location	Hill height h_0 [~~D~~D]	Hill width σ [~~D~~D]	σ/h_0 [-]	Surface roughnes z_0 [m]	Control/type of simulation
A0	Flat	0	-	-	0.001	C_P-λ-θ surface, no control
B0	Foot of hill	1	1.5	1.5	0.001	C_P-λ-θ surface, no control
C0	Top of hill	1	1.5	1.5	0.001	C_P-λ-θ surface, no control
A1	Flat	0	~~0~~ -	-	0.001	Controller
B1	Foot of hill	1	1.5	1.5	0.001	Controller
C1	Top of hill	1	1.5	1.5	0.001	Controller
C2	Top of hill	1	1.5	1.5	0.1	Controller
C3.1	Top of hill	0.75	1.5	2.0	0.001	Controller
C3.2	Top of hill	0.50	1.5	3.0	0.001	Controller
C3.3	Top of hill	0.25	1.5	6.0	0.001	Controller
C4.1	Top of hill	0.75	1.125	1.5	0.001	Controller
C4.2	Top of hill	0.50	0.75	1.5	0.001	Controller
C4.3	Top of hill	0.25	0.375	1.5	0.001	Controller
C4.4	Top of hill	0.125	0.1875	1.5	0.001	Controller

2.5 Turbulence model, inflow, boundary conditions and solver

The simulations are performed as RANS simulations using the k-ε-fp model (van der Laan et al., 2015b) as closure model. The standard model coefficients are left unaltered and the inflow is described by the analytical log-law solutions for the velocity U, the turbulence kinetic energy k and the dissipation ε (van der Laan et al., 2015a)

$$U = \frac{u_*}{\kappa}\log\left(\frac{z+z_0}{z_0}\right), \quad k = \frac{u_*^2}{\sqrt{C_\mu}}, \quad \varepsilon = \frac{u_*^3}{\kappa(z+z_0)}, \tag{12}$$

with the friction velocity u_* and the von-Kármán constant κ. It is important to mention that the level of turbulence intensity is independent of the friction velocity, which is varied in order to change the ~~hubheight~~ hub height velocity.

The described inflow is set as a boundary condition at the inlet and at the top of the domain in order to maintain the logarithmic profile in the absence of obstacles. At the outlet, a zero-velocity gradient condition is imposed, and at the bottom, a rough wall boundary condition as described by Sørensen et al. (2007) is used. The lateral boundaries are periodic.

The steady RANS equations are solved using the incompressible finite-volume solver EllipSys3D (Michelsen, 1992, 1994; Sørensen, 1995) ~~is used to solve the incompressible Navier Stokes equation in finite-volume formulation in a procedure similar to~~ using a modified version of the SIMPLEC algorithm to enforce pressure-velocity coupling (Kolmogorov et al., 2015).

2.6 Sensitivity analysis

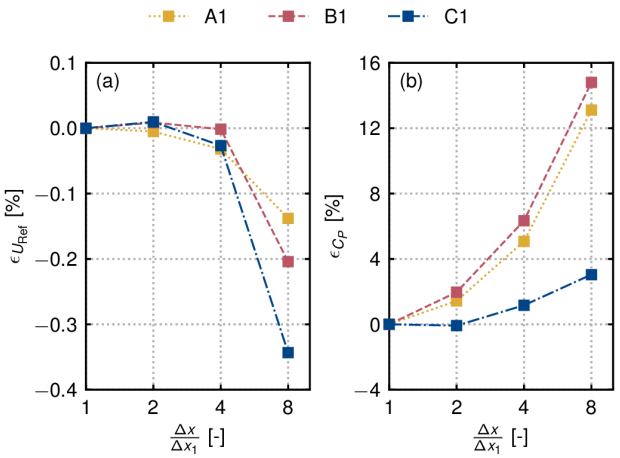

Figure 2. Change $\epsilon = \frac{f - f_1}{f_1}$ of the variable f relative to the solution on the finest grid f_1 when increasing the cell side length Δx for the three considered domain types. **(a)** U_{Ref}, and **(b)** C_P.

The sensitivity of the simulation setup to the cell size is analyzed. We evaluate the variation of the reference velocity U_{Ref} and of the power coefficient C_P, because they are the most important variables characterizing power performance. The grid is structured; therefore, the cell size is varied by combining several cells into a single cell, or, in other words, by running at a lower grid resolution. In Fig. 2, the results are reported as changes in U_{Ref} and C_P relative to the ~~SIMPLE-algorithm (Sørensen, 2018).~~ solution obtained on the finest grid, which is also the grid we use in this work. U_{Ref} varies by less than 0.01 % when changing the resolution from the finest grid to one level coarser. Increasing the cell side length by a factor of eight affects the reference velocity in all cases by less than 0.4 %. When the turbine is operating with a controller, the power coefficient varies by less than 2 % between the two finest grid levels. At the coarsest investigated grid, the power coefficient is up to 15 % higher.

The impact of the domain size on the results has been studied in a previous work. For a turbine located on a hill, increasing the cross-sectional area of the computational domain by a factor of eight results in a change in the disk-averaged velocity of less than 0.1 % for a fixed C_T (Zengler et al., 2024).

3 Results

The results are organized by first presenting ~~the prescribed~~ undisturbed velocity profiles at the respective turbine locations, then the obtained C_P-λ-θ surfaces ~~obtained at the three considered locationsand~~ at these locations, analyzing the differences in ~~$C_{P,\mathrm{max}}$~~$C_{P\mathrm{max}}$, λ_{opt}, and θ_{opt}. The controller constant k is set using the values of ~~$C_{P,\mathrm{max}}$~~ $C_{P\mathrm{max}}$ and λ_{opt} obtained at the flat location (**A0**). ~~After this~~Next, power curve calculations are performed at all three turbine positions ~~with~~ for this controller, and control-relevant quantities ~~like λ and induction factors are discussed in this context.~~ and resulting flow fields are presented.

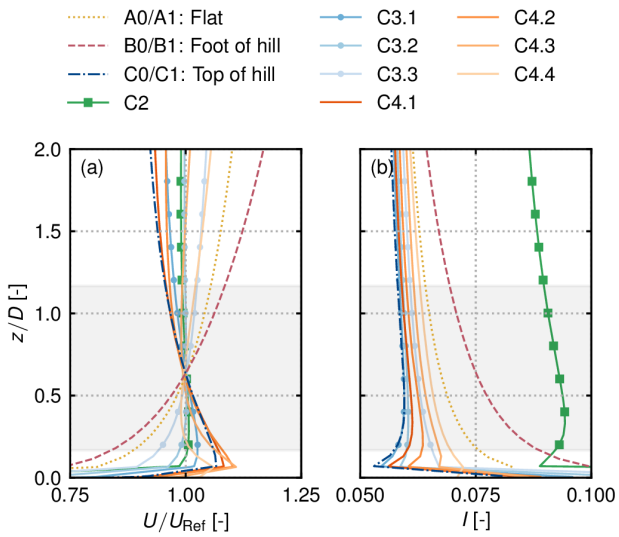

Figure 3. Undisturbed normalized velocity profiles U at the rotor position for all considered cases in **(a)** and turbulence intensity I in **(b)**. Grey areas indicate the rotor position. In all cases, the inflow profiles of the simulations are identical to the flat terrain profile, except for case **C2**, which has a higher surface roughness.

3.1 ~~C_P-λ-θ surfaces~~

3.1 Freestream velocity and turbulence intensity profiles at the rotor position

In Fig. 3, the undisturbed velocity profiles and turbulence intensity profiles at all considered turbine positions are shown. For all cases, the inflow profiles are identical to the profiles in flat terrain (**A0/A1**) corresponding to a neutral inflow at $z_0 = 0.001$ m as described by Eqs. (12). Only for **C2** the inflow profiles are different, due to the higher surface roughness of $z_0 = 0.1$ m.

In flat terrain, the rotor-averaged turbulence intensity is 6.8 %. At the foot of the hill, the shear of the velocity profile is slightly higher than in flat terrain, and also the turbulence intensity is higher at 7.5 %. On top of the hill (**C0/C1**), negative shear due to the hill-induced speed-up close to the surface occurs, and the turbulence intensity is only 5.9 %. The cases **C3.X** - **C4.X** are mostly enclosed by the flat terrain profiles and the highest-hill (**C0/C1**) profiles. With decreasing height, the profiles generally converge towards flat terrain. The hills of **C4.X** are steeper than the hills of **C3.X**, leading to a stronger speed-up close to the ground and higher levels of turbulence intensity. The case **C2** shows very little shear over the rotor area and the highest levels of turbulence intensity of 9.2 %. The different shear profiles result in different distributions of kinetic energy across the rotor area, but this bias is accounted for by calculating the rotor-equivalent wind speed (Eq. (10)) as a reference wind speed. Since turbulence intensity also affects turbine power performance, we assess the bias in the simulation results introduced by the different levels of turbulence intensity at the different turbine positions. The impact of turbulence intensity I on power can

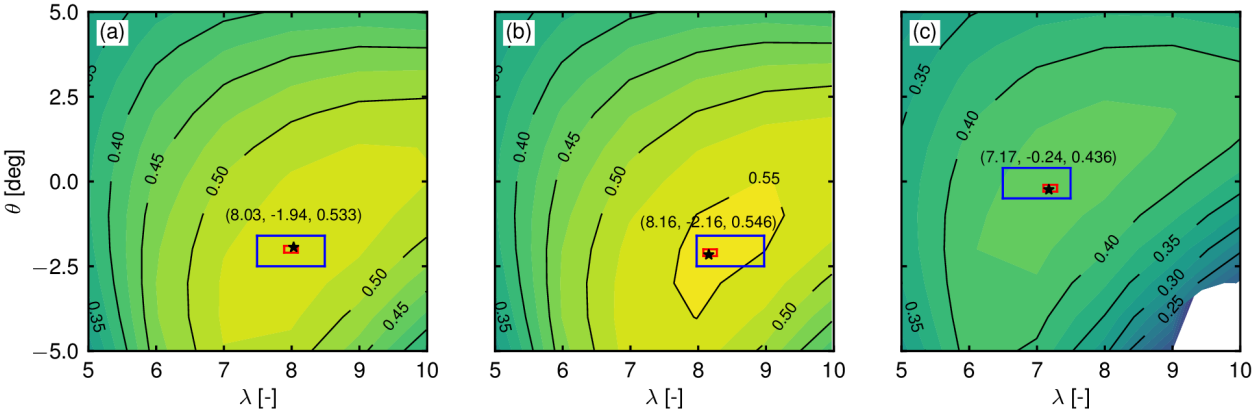

Figure 4. C_P ~~surfaces~~ surfaces obtained in **(a)** a flat domain ~~(~~**A0**, ~~left),~~ **(b)** on the foot of the hill ~~(~~**B0** ~~, center)~~ and **(c)** on top of the hill ~~(~~**C0**~~, right)~~. ~~White~~ Black stars indicate the point of optimal power performance. ~~Iso-curves~~ These discrete optima are found by a nested grid search: the outer meshgrid has a spacing of $\Delta\lambda = 1$ and $\Delta\theta = 1$ deg, within the ~~undisturbed flow velocity magnitude in~~ blue square the ~~graphic illustrate regions of speed-up in~~ grid spacing is $\Delta\lambda = 0.1$ and $\Delta\theta = 0.1$ deg and within the ~~vicinity of~~ red square the ~~hill~~spacing is $\Delta\lambda = 0.02$ and $\Delta\theta = 0.02$ deg.

be estimated as (Elliot and Cadogan, 1990)

$$P(I) = P_{I=0}\left(1 + 3I^2\right). \tag{13}$$

Based on the rotor-average of the turbulence intensity, it is expected that when neglecting any other effects, such as streamwise flow development, the power and also the power coefficient at the foot of the hill is approximately 0.3 % higher than in flat terrain at the same undisturbed wind speed and approximately 0.4 % lower on top of the hill for the lowest case of turbulence intensity. In case of **C2**, we expect an impact of 1.2 %.

3.2 C_P-λ-θ surfaces

Figure 4 shows C_P as a function of the blade pitch angle and the tip-speed ratio ~~(~~for cases **A0**, **B0**, and **C0**~~)~~. The surfaces are obtained on a coarse grid with $\Delta\lambda = 1$ and $\Delta\theta = 1$ deg, and the maxima are found by ~~cubic spline interpolation. In addition, at the optimal pitch in flat terrain (- 1.8 deg), the C_P-λ curves for all locations are simulated~~ a nested grid search, where, based on the discrete maximum on the coarse grid, a finer region is defined. In this finer region, a surface with spacing $\Delta\lambda = 0.1$ and $\Delta\theta = 0.1$ deg is simulated and based on the obtained maximum within this region, an even finder grid with $\Delta\lambda$ =~~0.5. These curves will be later shown in Fig. 6.~~ 0.02 and $\Delta\theta = 0.02$ is simulated. The final maxima are, in all cases, within the finest regions and not on their boundaries, ensuring that the optimum is actually in this region. On top of the hill, ~~sufficient convergence~~ a sufficiently converged flow solution could not be reached for cases of $\lambda = 10$ and θ = -5, -4 deg~~.~~, due to the high loading on the flow. The combination of a high disk-based thrust coefficient ($C_T > 1$) and a deceleration of the flow behind

the ridge leads to oscillations in the solution, suggesting that it may be unsteady and not solvable with a steady-state RANS model.

In flat terrain, the optimal C_P is ~~0.543~~ 0.533 at a blade pitch angle of $\theta =$ ~~-1.8~~ -1.94 deg and a tip-speed ratio of ~~8.1~~8.03. These values differ from the ones specified for the DTU 10 MW RWT ~~Bak et al. (2013), ($C_P \approx 0.474$, $\theta = 0.0$, $\lambda = 7.5$)~~ (Bak et al., 2013), which can be mainly attributed to ~~the well-known fact that the induction in the rotor plane is usually over-predicted in AD simulations (Mikkelsen, 2004; Zengler et al., 2025a). As a consequence, the power coefficient is higher, and the blades need to be pitched back more to account for the change of the local flow angle.~~ additional load constraints considered when designing the original controller for the DTU 10 MW RWT. Reducing loads requires positively pitching the blades, explaining why the original tuning resulted in a higher pitch angle.

When the turbine is located at the foot of the hill, the maximum power performance increases by ~~3.5 %~~2.46 %, accompanied by a decrease of optimal pitch (~~-2.1~~ -2.16 deg) and an increase of the tip-speed ratio (~~8.3~~8.16). At the top of the hill, the opposite is true. The maximum power coefficient decreases by ~~20.0% to a value of 0.437~~ 18.25 % together with an increase of pitch ~~(-0.4 deg)~~ (-0.24 deg) and a decrease of the tip-speed ratio (~~7.2). The indicated~~ 7.17). Both on top of the hill and at its foot, the change in C_P is significantly greater than what one would expect due to the different levels of turbulence intensity at the position of the turbine, as discussed in the previous section.

The undisturbed velocity contours in Fig. ~~4~~ 1 show that the flow accelerates behind the turbine located at the foot of the hill, while it decelerates behind the turbine at the hill top. In line with previous research (Revaz and Porté-Agel, 2024; Troldborg et al., 2022; Dar et al., 2023), deceleration results in a decrease in power performance while acceleration results in an increase. The presented C_P~~surfaces~~ -surfaces indicate that there is no possibility of operating at the same optimal power coefficient as in the flat case when the turbine is operating on the hill, regardless of pitch and tip-speed ratio, because the ~~available power~~ power coefficient is limited by the flow development. However, this does not necessarily mean that placing a turbine on top of a hill leads to worse power performance in absolute numbers, because wind speeds on top of hills are often higher. The actual benefit one can expect by placing a wind turbine on a hill will be discussed in ~~See~~Sect. 4.3.

3.3 Simulations with active controller

The pitch and torque controllers are tuned based on the steady-state optimal performance in flat terrain (**A0**) ~~. The torque constant (Eq. **??**) is set to $k = 11 \times 10^6$ Nms^2 and the rated generator speed is set to 1.0 rad^{-1}. The minimum pitch the pitch controller can operate at is set to -1.8 deg. Because the pitch controller is a PI controller that tracks the error between generator speed and rated generator speed, the negative error below rated wind speed will result in a negative pitch signal, which will saturate at this minimum pitch of -1.8 deg. As a consequence, in region two, the pitch is held constant at -1.8 deg, which can also be seen in Fig. **??** (b).~~ and the resulting control constants are listed in Table 1. Simulation results with controller are presented in two steps. First, quantities characterizing performance, such as power, C_P and λ , are presented; second, the resulting flow fields around the turbine are shown.

With the calibrated controller, the power curves are ~~run for an increasing wind speed, which is achieved~~ obtained by varying the friction velocity u_* in Eq. (12).

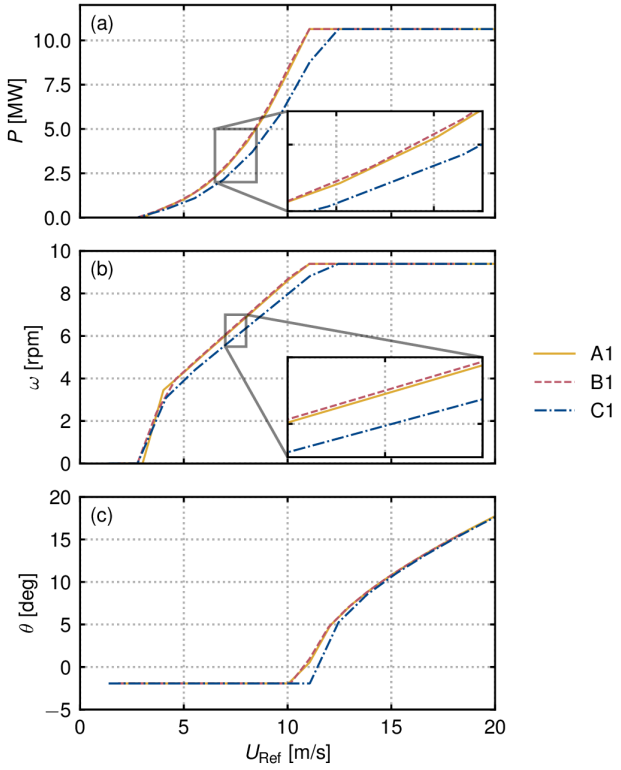

Figure 5. Power curves obtained with the controller in flat terrain (**A1**), ahead of the hill (**B1**) and on top of the hill (**C1**) with the power in **(a)**, the respective rotor speed in **(b)** and the blade pitch in **(c)**.

~~The key simulation results at the three positions~~ The results for flat terrain, ahead of the hill, and on top of the hill are shown in Fig. ~~6~~ 5 with the power shown in panel (a). ~~All power curves show the three typical distinct regions in which a turbine operates: region one, below cut-in wind speed, where no energy is produced, region two, where the primary objective is the maximization of energy production, and region three, where energy extraction is limited to the rated power.~~ The turbine on top of the hill produces significantly less energy below rated wind speed than the one in flat terrain for the same undisturbed ~~rotor~~ wind speed at the rotor, while the one at the hill's foot produces slightly more energy for the same undisturbed rotor wind speed. Note that although the wind speed changes, Reynolds-similarity leads to the development of similar flow features independent of the wind speed (van der Laan et al., 2020), which is why the induction below rated wind speed is unaltered by the inflow velocity. Above rated conditions, all turbines produce the same power as a consequence of the pitch controller aiming ~~at maintaining~~ to maintain a certain rotor speed independently of the ~~energy content of~~ maximum available power in the flow. ~~Although this work does not focus on region 2.5, one can see thatits onset is delayed for the turbine on the hilltop due to a lower rotational speed for a given undisturbed rotor wind speed.~~ The corresponding rotor speed, shown in Fig. 5 (b), exhibits the same behavior as the power, being slightly higher ahead of the hill and significantly lower at the hilltop. Inspection

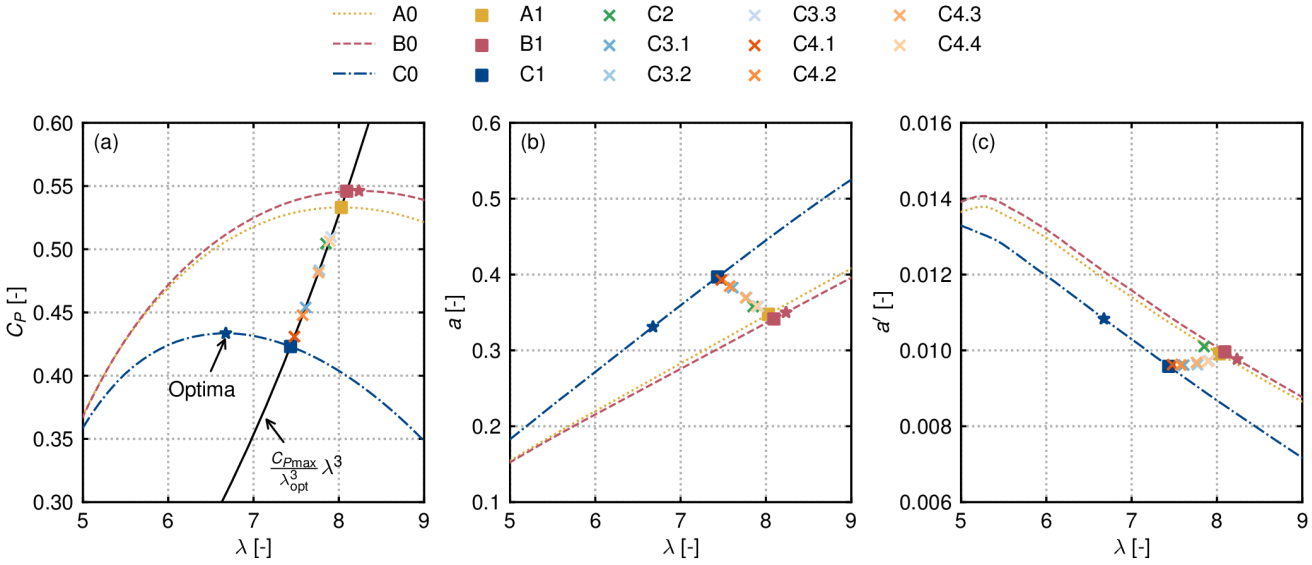

Figure 6. Simulation results for the controlled turbine placed at the ~~three~~ different positions~~(**A1, B1,C1**)~~: ~~(a) Power curves, (b)~~ **(a)** C_P-λ curves with control curve in solid black, steady state operational points below rated wind speed marked as crosses and discrete maximum C_P marked by stars, ~~(c)~~ **(b)** induction curves and operational points with $a = 1 - u_R/U_{\text{Ref}}$ where u_R is the kinetic energy mean over the rotor calculated like U_{Ref} in Eq. (10) and ~~(d)~~ **(c)** tangential induction ~~$a' = u_{R,t}/(\omega r)$~~ a' evaluated as azimuthal mean at $r = 0.75R$.

of the blade pitch in Fig. 5 (c) shows that, below rated conditions, the pitch is identical for all cases, settling at -1.94 deg. When reaching rated conditions, the controller of the turbine ahead of the hill starts to pitch at lower wind speeds than in flat terrain, whereas the opposite is true for the turbine on the hilltop. This can be attributed to the different rotor speeds, which serve as an input signal for the pitch controller. Overall, the reported trends are in agreement with the results by Troldborg et al. (2022).

~~Figure 6 (b~~Turning towards the non-dimensional quantities characterizing turbine operation in region 2, Fig. 6 (a) shows the C_P-λ ~~curve,~~ curves of **A0**, **B0**, and **C0** at θ = -1.94 deg, including the points where the torque controller settles in region ~~two~~ 2 during the power curve calculation for all considered simulations. Regardless of the turbine position, the controller settles at the intersections ~~between~~ of the control curve given by Eq. (~~5~~7) and the respective performance curves ~~. Especially from the case on top of the hill~~as it is shown for the cases **A0/A1**, **B0/B1**, and **C0/C1**. Specifically for the case **C1**, it becomes apparent that this intersection does not necessarily represent the point of maximum power ~~capture~~performance. In numbers, at the foot of the hill, the ~~turbine produces 2.4% more power~~ C_P at which the controller settles is 2.40 % higher than in flat terrain~~with the same undisturbed reference wind speed~~, while it ~~produces 20.6% less power~~ is 20.63 % lower on top of the hill. If the torque constant were tuned to match the optimal tip-speed ratio in both cases, the gain ahead of the hill would be around 2.45 % while on top of the hill, the loss would reduce to 18.67 %. Adjusting also the blade pitch would further improve the results as shown in Fig. 4.

Figure 6 (~~c~~b) shows the axial induction as a function of λ. At the foot of the hill, it is always lower than in flat terrain, while on top of the hill, it is always higher, corresponding to a higher and lower C_P, respectively. ~~It is observed that at~~ At the top of the hill, the optimal tip-speed ratio would be approximately 6.7, resulting in a ~~decreasing~~ lower induction relative to the flat case. ~~On the other side~~However, the controller settles at a tip speed ratio of ~~7.5~~ 7.4 with an increased induction relative to the flat case. There is a general trend that for the controlled turbine, the induction decreases with an increasing tip-speed ratio.

In Fig. 6 (~~d~~c), the azimuthally averaged tangential induction $a' = u_{R,t}/(\omega r)$ evaluated at 0.75 ~~R~~ R is presented. The a'-λ curves show an opposite trend to the a-λ curves. The tangential induction ~~in general~~ generally decreases with an increasing tip-speed ratio; however, for a given tip-speed ratio, it is always lower at the top of the hill and higher ahead of the hill, ~~so following the opposite trend compared to the~~ which is opposite to the trend followed by the axial induction. In comparison to the axial induction, the tangential induction of the controlled cases ~~(marked by crosses)~~ seems to stay rather constant during operation at the three different locations. Only a small trend can be observed: Ahead of the hill, the tangential induction increases, while it decreases on top of the hill. ~~In See~~An outlier is case **C2**, the one with the higher surface roughness compared to case **C1**, showing a higher tangential induction than all other cases. In Sect. 4.1, it will be discussed whether tangential induction is expected to stay constant during torque control. There, the radial distributions of axial and tangential induction will also be shown.

After presenting performance quantities only, we will now extend the results by also presenting the respective flow fields for all cases. Figure 7 shows velocity contours in the x-z plane through the rotor center. Velocities are normalized by the undisturbed velocity at the turbine position. Note that in all cases, the x coordinate is relative to the position of the rotor.

Case **C1** in Fig. 7 shows, that the flow speed is lower everywhere around the turbine, while for case **B1**, one can see that the hill behind the accelerates the flow around the turbine. Comparing cases **C1** and **C2**, the velocity deficit in the wake is lower in the latter case. It has already been noted by Revaz and Porté-Agel (2024), that there is a strong negative correlation between the maximum velocity deficit in the wake and the respective power performance, although there are exceptions specifically for cases where flow separation occurs. A comparison of the second and third row of Fig. 7 shows that at a given hill height, the power performance is higher for the wider hill or the lower maximum slope, respectively, which is in agreement with Revaz and Porté-Agel (2024) and Zengler et al. (2024). Comparing the panel of **C3.3** with the panel of **A1** already indicates how an increasing widening of the hill leads to a flow field around the turbine converging towards a field close to flat conditions.

Figure 8 shows the undisturbed and disturbed velocities at constant height above ground (hub height). The figure reveals several noteworthy characteristics: First, it is observed that the undisturbed flow does not accelerate at the turbine position ahead of the hill, but rather slightly behind it. This indicates that predicting power performance bias solely by evaluating acceleration at the turbine position is insufficient, and that the flow field downstream also needs to be considered, as previously mentioned (Zengler et al., 2024). A comparison of cases **C1** (low roughness) and **C2** (high roughness) shows a nearly identical development of the undisturbed hub-height velocity ahead of the hill, whereas the deficit behind the hill is markedly deeper in **C2**. When the turbine is operating, the opposite behavior is observed. This indicates a non-linear interaction between turbine, flow and terrain. Comparing cases with the same hill height but different widths (**C3.1** - **C3.3** and **C4.1** - **C4.3**) shows that, at a

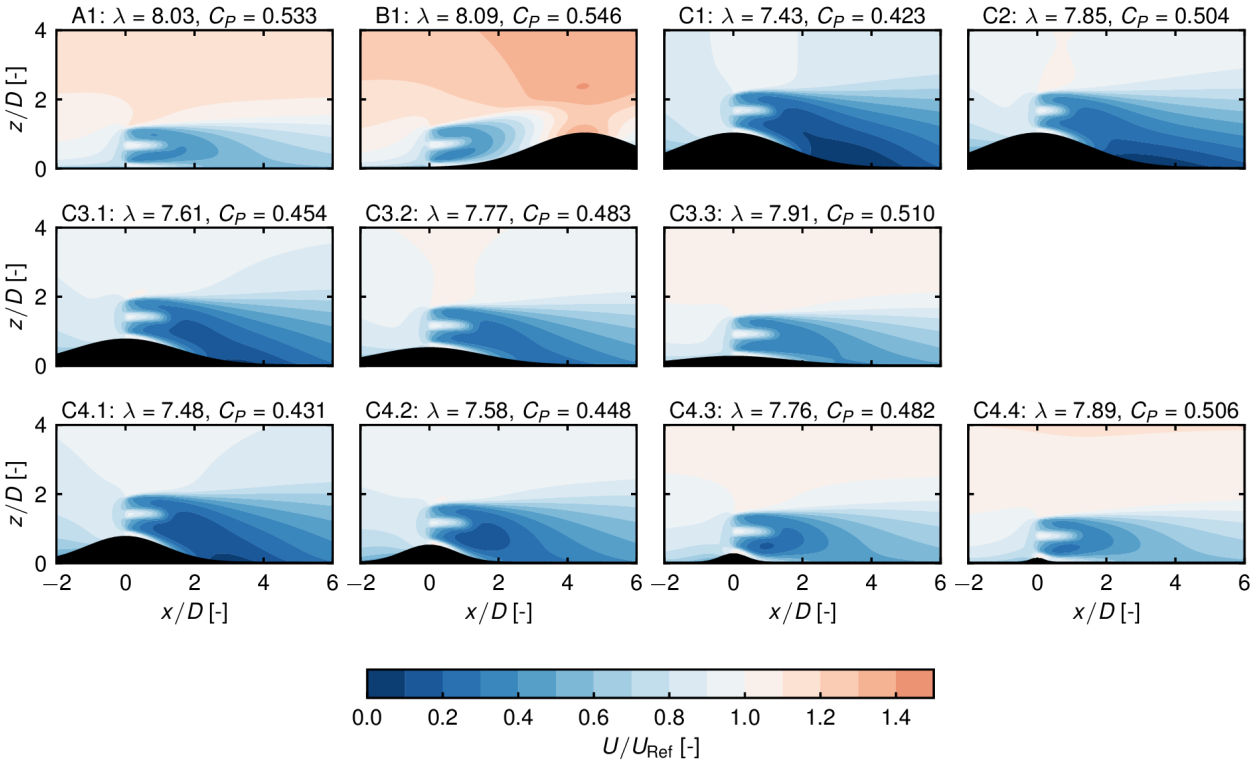

Figure 7. Flow fields developing around the turbine operating with an active controller for the investigated cases.

given hill height, the flow field differs only near the turbine, with stronger acceleration and deceleration for the narrower hills. In all cases, there is a speed-up directly at the turbine position when the turbine is operating (also visible in Fig. 7). This is a consequence of the missing nacelle, which leads to a channeling of the flow through the rotor center.

4 Discussion

The previous section showed that the power performance is markedly affected when a flat-terrain-designed turbine operates under complex-terrain conditions. This is primarily a consequence of the flow physics as seen in Fig. 4. Additionally, the controller leads to suboptimal performance in these situations as seen in Fig. 6 (~~b~~a).

~~Next~~Now, we characterize the behavior of the torque and pitch controllers. ~~It is furthermore asked how strong the deterioration of the actual power is, considering the effect of higher wind speeds on top of the hill relative to flat terrain~~Furthermore, we investigate how much the turbine's actual power output on the hilltop differs from what would be expected from the speed-up alone. Lastly, the limitations of the present study are discussed.

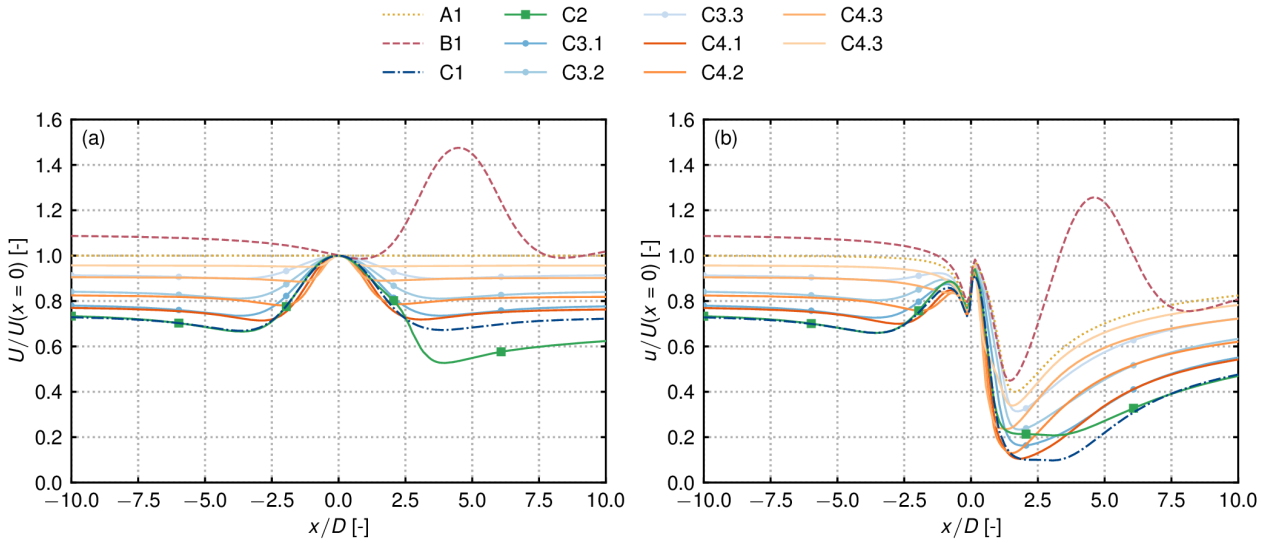

Figure 8. Velocity at hub height (terrain-following) without turbine operating in **(a)** and with turbine operating in **(b)** with the turbine being located at $x = 0$.

4.1 Role of torque controller

Figure 6 (~~b~~a) shows that the torque controller follows its prescribed control curve as expected, even when the surrounding flow field changes to conditions the controller was not calibrated for. On the one side, this is not surprising, because ~~eventually a torque controller~~ c.f. Eq. (7) the torque controller effectively enforces

$$\frac{C_{P,\max}}{\lambda_{\text{opt}}^3} = \frac{C_P}{\lambda^3} \tag{14}$$

for any operational state ~~(as seen in Eq. (5))~~ with the left-hand side being constant and calibrated, for example, for flat terrain in our case. On the other hand, this relation does not directly yield insights into how a ~~or~~ and the local a' change due to ~~the effect of complex terrain~~complex terrain, which will be analyzed in the following.

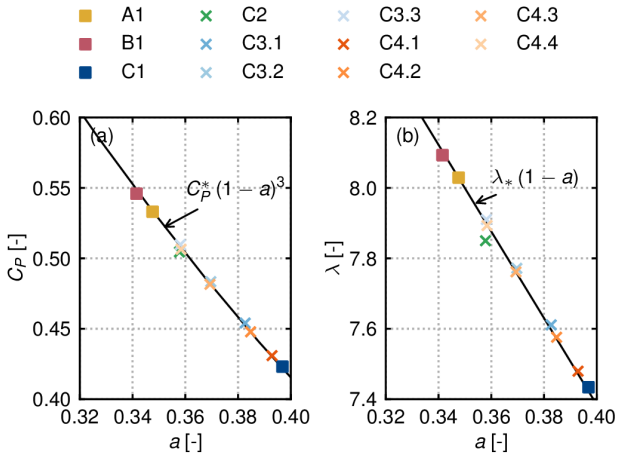

Figure 9. Power coefficient in **(a)** and tip-speed ratio in **(b)** as a function of the induction in flat terrain, ahead of the hill and on top of it together with Eq. (21) and Eq. (23) using $C_P^* = 1.92$ and ~~the points of optimal operation at every position~~ $\lambda_* = 12.31$.

4.1.1 Impact on axial induction and performance coefficients

We formulate the torque control strategy based on the velocity at the disk during operation. For this purpose, we introduce the operational power coefficient, thrust coefficient, and tip-speed ratio as follows

$$C_P^* = \frac{P}{\frac{1}{2}\rho u_D^3 A}\frac{P}{\frac{1}{2}\rho u_R^3 A} = C_P\left(\frac{U_{\mathrm{Ref}}}{u_D}\frac{U_{\mathrm{Ref}}}{u_R}\right)^3, \tag{15}$$

$$C_T^* = \frac{T}{\frac{1}{2}\rho u_D^2 A}\frac{T}{\frac{1}{2}\rho u_R^2 A} = C_T\left(\frac{U_{\mathrm{Ref}}}{u_D}\frac{U_{\mathrm{Ref}}}{u_R}\right)^2, \tag{16}$$

$$\lambda_* = \frac{\omega R}{u_D}\frac{\omega R}{u_R} = \lambda\frac{U_{\mathrm{Ref}}}{u_D}\frac{U_{\mathrm{Ref}}}{u_R}, \tag{17}$$

where ~~u_D~~ u_R is the flow in the turbine plane during operation, calculated ~~similarly to~~ using Eq. (10). The optimal power operation is then reformulated as

$$P_{\max} = \frac{1}{2}\rho\pi R^2 C_{P,\max} {u_D}^3 = \underbrace{\frac{1}{2}\rho\pi R^5 \frac{C_{P\max}^*}{\lambda_{*\mathrm{opt}}^3}}_{k}\omega^3 \tag{18}$$

with the control constant k being the same as the one defined in Eq. (3) because u_D and U_{Ref} cancel out in both equations, respectively. This shows that optimal control actually enforces an equilibrium between power and the velocity in the turbine plane during operation, independently of the ~~free-stream~~ freestream velocity. This makes intuitive sense because eventually the forces and moments on the turbine blades purely depend on what the local flow is at the disk. In fact, the only ~~thing~~

quantity that a torque controller keeps constant is the ratio between torque and rotor speed squared, regardless of what velocity is used as reference velocity, as seen in Eq (5). Because rotor speed and disk velocity are related by a constant during torque control in order to keep the local flow angles constant, an equilibrium between power and disk velocity during operation is also achieved (Zengler et al., 2025b). Thus, a turbine calibrated for a certain operational point keeps C_P^* constant and not C_P.

~~In our simulations, we find that C_P^* and λ_* are practically constant; $C^*_{P,\max} = 1.92 \pm 0.0076$ and $\lambda_{*,\mathrm{opt}} = 12.36 \pm 0.016$.~~ We find for all cases $C_P^* \approx 1.92$, $C_T^* \approx 2.27$, and $\lambda_* \approx 12.31$.

The introduction of certain non-dimensional quantities hides the actual physics~~happening here~~. The relation between C_T and a changes in terrain, but not the relation between the local blade forces and velocities. To circumvent this problem, one could either use quantities for non-dimensionalization that do not change, such as ~~u_D~~ u_R in our case, or work exclusively in dimensional form. ~~This, on the other hand, would make it difficult to compare results.~~

Returning to torque control, for the optimal thrust, it follows that

$$T_{\mathrm{opt}} = \frac{1}{2}\rho\pi R^2 C_{T,\mathrm{opt}} {}^{*} u_D^2 = \underbrace{\frac{1}{2}\rho\pi R^4 \frac{C^*_{T\mathrm{opt}}}{\lambda^2_{*\mathrm{opt}}}}_{\text{constant}} \omega^2, \tag{19}$$

from which ~~it can be furthermore deducted that~~ the following can be deduced

$$\frac{C_T}{\lambda^2} = \frac{C_T^*}{\lambda_*^2} = \text{constant}. \tag{20}$$

How do these considerations now affect a, a', C_P, and C_T during torque control? Based on Eqs. (15) ~~, (16), and (~~ (17) the following relations are obtained

$$C_P = C_{P,\max} {}^{*} (1-a)^3, \tag{21}$$

$$C_T = C_{T,\mathrm{opt}} {}^{*} (1-a)^2, \tag{22}$$

$$\lambda = \lambda_{*,\mathrm{opt}} {}_{*} (1-a). \tag{23}$$

~~In Fig. 9 ,~~ Figure 9 shows Eqs. (21) and (23) ~~are shown~~ alongside the simulation results ~~showing~~ and reveals that indeed the turbine always operates on these curves. At this point, it is worth taking a look at control strategies, which set blade forces based on ~~u_D~~ u_R and C_T^* (van der Laan et al., 2014; Meyers and Meneveau, 2010; Calaf et al., 2010). The current findings show that classical torque control is equivalent to these strategies, keeping C_T^* and C_P^* constant, rather than C_T and C_P. ~~This~~ , which has also been shown ~~before (Zengler et al., 2025b).~~ previously (Zengler et al., 2025b). This is an important finding, as it shows, using disk-based quantities for a simplified control yields identical results as k-ω^2 control in region 2 of the power curve, irrespectively of the development of the flow field. It must be noted though, that this does not apply to region 3, where the modified induction in non-uniform flows can lead to different pitch signals and consequently differing power performance.

4.1.2 Impact on tangential induction

~~The question of~~ In the following the reason why the tangential induction a' ~~shown in Fig. 6 (d)seems to be independent of the effects of the complex terrain, when the other quantities are affected by it, is so far unanswered. In order to answer this, a local analysis of the blade forces is carried out in appendix A. By considering only the effect of lift forces on the flow and neglecting drag, it can be shown that a'~~, as shown in 6 (c), is only vaguely sensitive to terrain effects will be explained. In appendix A, it is shown that by disregarding drag, the local tangential induction can be calculated as

$$a'(\mu) = \frac{1}{2}\left(-1 + \sqrt{1 + \frac{C_t(\mu)}{\lambda^2 \mu^2}}\right), \tag{24}$$

with the non-dimensional radial coordinate $\mu = r/R$ and the local thrust coefficient C_t. From this equation, it is evident that a' only depends on the local blade forces and rotor speed. The reference velocity used for normalization of λ and C_t can be omitted from the equation, because C_t is normalized by U_{Ref}^2 and λ by U_{Ref}, so when dividing C_t by λ^2, U_{Ref} cancels out. It was shown in Eq. (20) that the ratio $\frac{C_T}{\lambda^2}$ is constant for a torque controller. Based on this, it can ~~therefore~~ now be argued that the local version of that ratio $\frac{C_t(\mu)}{\lambda^2}$ should be constant as well, as long as changes in the flow state due to terrain are uniform over the disk. This explains why a' is independent of the effects of complex terrain in region ~~two~~2, although rotor speed and thrust change; it is simply a consequence of the torque control. In Fig. 10 (a) and (b), the local axial and tangential inductions are shown~~as function of radial position along the blade as well as the angle of attack α in (c). Indeed~~. While the axial induction varies significantly between the presented cases, the tangential induction is nearly identical in all cases. ~~Only close to the root are deviations~~ Deviations between the cases ~~visible~~are only visible close to the root. A possible explanation for this is that in this region drag plays a significant role, also affecting the tangential induction.

Lastly, Fig. 10 (c) shows the local angle of attack α. Since the local tip-speed ratio λ_* and flow angles remain constant, it does not come as a surprise, that the angles of attack do not change during torque control, supporting the analysis in the previous section.

In summary, a torque controller enforces C_P^*, C_T^*, and λ_* to stay constant. A consequence is that also a' is constant, which only depends on the local forces and flow. Because of the changing optimal inflow angles in complex terrain, a torque controller tuned for flat terrain cannot operate optimally with this strategy.

4.1.3 Optimal performance

We briefly discuss how a controller would need to operate to always track optimal performance. From Eq. (23), one can see that the rotor speed at a given reference velocity (λ) decreases with a decreasing disk velocity (an increasing induction~~a~~). In Fig. ~~9~~ 6 (b), the optimal performance on top of the hill would be reached by reducing the induction and ~~also reducing~~ the tip-speed ratio. From a local perspective, this results in higher axial velocities and lower relative tangential velocities. As a consequence, the local flow angle and angle of attack increase when ~~not adjusting pitch~~ the pitch is not adjusted. However, as suggested by Fig. 4, ~~also~~ the pitch should also be modified to track optimal performance, which would eventually change the angle of attack.

Ahead of the hill, when the background flow is accelerating, the opposite is the case; to track optimal performance, the angle of attack would need to decrease. This observation is also in agreement with previous findings based on momentum theory

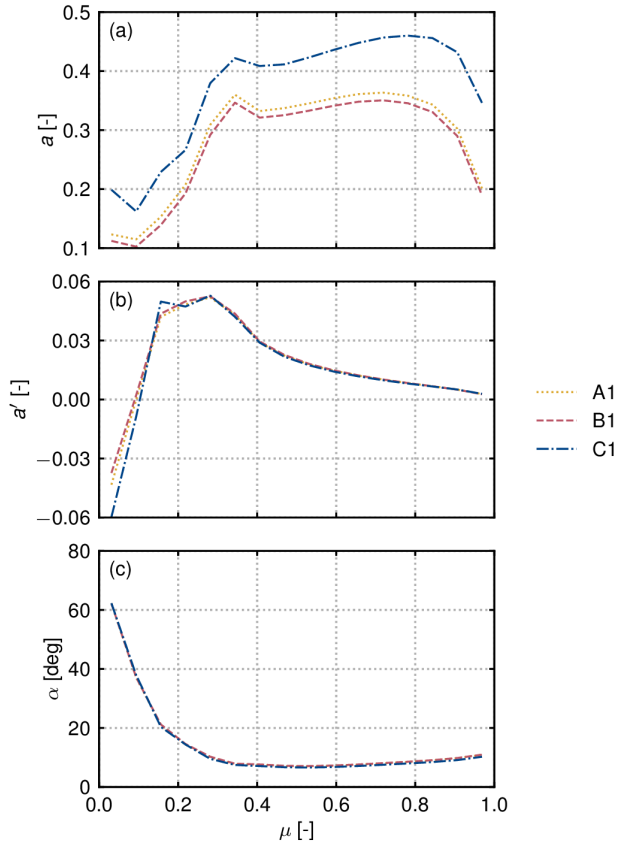

Figure 10. Azimuthally averaged axial induction ~~(a)~~**(a)**, tangential induction ~~(b)~~**(b)**, and angle of attack α ~~(c)~~ **(c)** shown as a function of nondimensional radial position $\mu = r/R$.

(Zengler et al. (2025a), see also Eq. (B5)), which show that in a decelerating flow, the optimal performance would be reached at a lower induction, while in an accelerating flow, it would be reached at a higher induction. Without modification of the torque constant, a torque controller would therefore always operate below optimum in accelerating flow fields, because it effectively keeps flow angles constant instead of adjusting them to the flow conditions. Since blades are often designed to achieve the best two-dimensional polar lift-to-drag ratios at the angles of attack corresponding to region ~~two~~ 2 operation, torque control ensures that the airfoil sections are performing well from a two-dimensional perspective. The reason for suboptimal power performance is the changed (axial) induction response in accelerating flows.

A way of approaching this problem of suboptimal power performance outside the flat operating conditions would be to include control algorithms, which slowly modify the torque constant (and pitch) over time to reach optimal performance (see~~for example~~ , for example, extremum seeking control ~~, Creaby et al. (2009)~~(Creaby et al., 2009)). However, as Fig. 6 (b) indicates, the total gain in performance is rather low on a given curve. Also, the gradient $\frac{\partial C_P}{\partial \lambda}$ might not be very strong. In

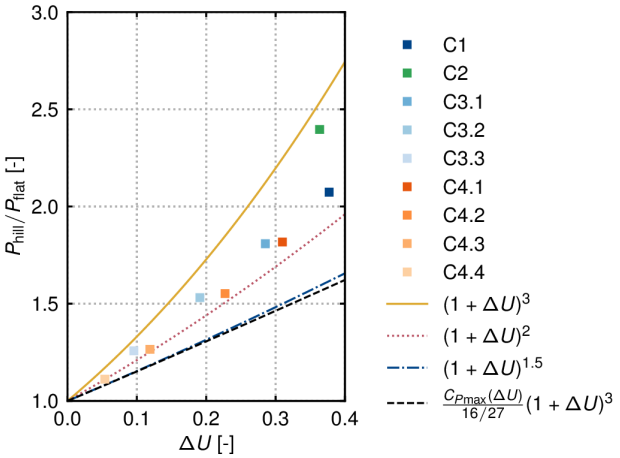

Figure 11. Expected and actual power at the top of the hill for different speed-up factors. The ~~variation in speed-up is reached by changing the roughness to 0.1 m (**C2**), varying the hill height and keeping the width constant (**C3.1-C3.3**), and by varying the hill height while keeping the ratio between width to height constant (**C4.1-C4.4**). The~~ turbines were simulated, including a controller, so the potential maximum power performance would be around one percent higher.

combination with varying atmospheric conditions, which are not part of this study, and also seasonal variations of the terrain surface, optimization of the torque constant might be difficult and the expected gain possibly small, if not even negligible.

~~In summary, a torque controller enforces C_P^*, C_T^*, and λ_* to stay constant. A consequence is that also a' is constant, which only depends on the local forces and flow. Because of the changing optimal inflow angles in complex terrain, a torque controller cannot operate optimally with this strategy.~~

4.2 Role of the pitch controller in region ~~two~~2

The pitch controller tracks the difference between the actual and rated rotor speed. In region ~~three~~ 3 of the power curve, this leads to the observed behavior that even in a non-uniform background flow, the same rated power is reached in the different cases. In region ~~two~~2, the pitch controller remains inactive, although Fig. 4 suggests that performance could be increased by adjusting the pitch. The reason for this is the implementation of the pitch controller as a PI controller. Below the rated wind speed, or rather the rated rotor speed, the difference between actual and rated rotor speed is negative, resulting in a negative pitch signal saturating at the minimum pitch independently of the flow state. Similarly to the torque controller, one could imagine an algorithm that modifies the minimum pitch seeking maximum power performance in region 2 of the power curve. However, in practice, it might again be difficult because of the small differences between optimal and actual pitch.

4.3 Speed-up factors

A common way to account for the effect of complex terrain is to use speed-up factors. Because power scales with the wind speed cubed in the flat terrain case, the effect of terrain on the power of a turbine is usually estimated as

$$P_{\text{hill}} \approx P_{\text{flat}}(1+\Delta U)^3, \tag{25}$$

with $\Delta U = (U_{\text{Ref,hill}} - U_{\text{Ref,flat}})/U_{\text{Ref,flat}}$ being a non-dimensional velocity speed-up factor. This estimate is only accurate as long as the actual power coefficient of the turbine is the same as that in the flat terrain case. However, as shown ~~before, when the turbine is located~~ above, placing the turbine on a hill ~~,~~ reduces the power coefficient ~~decreases~~ due to the streamwise ~~development of the flow behind the turbine~~evolution of the downstream flow. This raises the question of what is actually the maximum performance that can be reached by placing wind turbines on elevated spots, such as hills.

To ~~answer~~ address this question, we ~~consult the additional simulations mentioned at the beginning (C2~~analyze all simulations with the turbine located on top of the hill using the model by Zengler et al. (2025a). The model can predict the maximum power coefficient $C_{P\text{max}}$ as a function of the speed-up, ~~C3.1-C3.3, C4.1-C4.4) and use a model that incorporates the effect of streamwise velocity gradients on the power coefficient (Zengler et al., 2025a). By~~ ΔU, by assuming that the maximum deceleration behind the hill is ~~similar~~ comparable to the speed-up ahead of ~~the hill~~ it, and that the speed-up region is smaller than the region ~~where~~ in which the wake pressure equalizes with the surrounding pressure~~, the change of the maximum power coefficient as a function of the speed-up ΔU, i.e. $C_{P,\text{max}}(\Delta U)$, according to this model can be estimated, which~~ . This is outlined in ~~appendix~~ Appendix B in more detail. Because this model yields identical results to momentum theory for $\Delta U = 0$, the scaling of the power on a hill can be estimated to be

$$P_{\text{hill}} = P_{\text{flat}} \frac{C_{P,\text{max}}(\Delta U)}{16/27} \frac{C_{P\text{max}}(\Delta U)}{C_{P\text{max}}(\Delta U = 0)} (1+\Delta U)^3, \tag{26}$$

$$= P_{\text{flat}} \frac{C_{P\text{max}}(\Delta U)}{16/27} (1+\Delta U)^3, \tag{27}$$

$$\approx P_{\text{flat}}(1+\Delta U)^{1.5}, \tag{28}$$

with ~~the second~~ $C_{P\text{max}}$ calculated from Eqs. (B4) and (B6) and the third line being an approximation based on visual inspection of the resulting curves. This estimate requires that the flow recovers to the flat terrain-state directly behind the turbine, and can therefore be interpreted as a lower bound to the possible maximum power performance. To investigate ~~how the power changes~~ the power increase on top of the hill in the ~~simulations presented , the actual power increase is shown together~~ presented simulations, Fig. 11 compares the simulated power increase with the traditional cubic trend (Eq. (25)), the lower bound from Eq. (27) ~~, its approximation (~~and its approximation Eq. (28)~~), and~~ , as well as a quadratic scaling for reference~~in Fig. 11.~~ . It is important to keep in mind that the simulation results also include a controller; thus, the actual maximum available power is expected to be around one percent higher, as shown in Fig. 6 (~~b~~a).

As expected, the actual power increase on top of the hill does not follow a cubic trend, but is in all cases lower. When the flow separates behind the hill, as is the case for $z_0 = 0.1$ m (C2), and the velocity immediately behind the turbine does not decelerate

so strongly, the power is closer to the cubic relationship. The same conclusions can be made comparing simulations **C3.1**-**C3.3** with **C4.1**-**C4.4**. When the width does not change, the deceleration behind the turbine is weaker, and the respective power performance is higher. Reducing both width and height results in a more local speed-up followed by a strong deceleration. None of the presented cases seems to scale according to Eq. (27), ~~the scaling is always higher, rather than being close to a quadratic trend~~but rather mostly show a close to quadratic scaling. Only for very small speed-ups, the scaling seems to approach ~~the~~ our theoretical predictions. As outlined previously, this can be explained through the assumptions made for deriving Eq. (27), which requires a very local speed-up with immediate wake recovery. These observations suggest that if terrain and flow features in the vicinity of the turbine are more similar to flat terrain features, such as a very long hill or a separation bubble that delays deceleration, the maximum power coefficients are also similar, leading to a more cubic scaling of power. If this is not the case, and flow and terrain features vary on similar length scales as those of the turbine, a stronger influence on the power coefficient can be expected.

~~Based on this analysis , it is concluded thatplacing a wind turbine in a spot where the speed is locally highest is beneficial for power performance. However, the limitation of the free stream velocities in the wake region potentially~~ The above analysis shows that, although higher wind speeds at a hilltop lead to increased power output, flow deceleration reduces the achievable gain ~~from what is expected from~~ compared to that predicted by the classical cubic ~~relation (Eq. (25)).~~ scaling. In cases where turbines are located in smaller local free stream speed-up regions, the scaling ~~exponent from the simulations was closer to 2, with even slower (but still positive) scaling indicated by Eq. (27) by theoretical means.~~ is closer to quadratic and may theoretically be even lower.

4.4 Limitations

Although this work deals with complex terrain, the studied case of ~~a wind turbine~~ an AD on a quasi-two-dimensional Gaussian hill remains a significant simplification. The undisturbed flow field is quasi-two-dimensional and varies only in the vertical and streamwise direction. Furthermore, the effect of atmospheric stability was not included. It remains a subject for future studies how a three-dimensional, unsteady flow would interact with the wind turbine, and to what extent the result that optimal induction decreases in a decelerating flow and increases in an accelerating flow also holds there. In this light, it would also be important to apply a more sophisticated turbine model, such as an actuator line model or a fully resolved turbine model, which leads to a more accurate representation of the local blade flow. This study focused on k-ω^2 control only, however other approaches to maximize power performance in region 2 such as tip-speed ratio tracking (Abbas et al., 2022) exist as well and it would be of interest how these would perform in complex terrain conditions.

5 Conclusions

Wind turbine performance in complex terrain is affected by a streamwise non-uniform flow field, resulting in changing limits of maximal energy extraction and by the control algorithm, not capable of adjusting properly to the physics caused by the modified flow conditions. It was shown that a torque controller keeps thrust and power coefficient based on the disturbed flow

field constant, which do not necessarily correspond to the point of operation, which yields maximum power performance in non-uniform flow fields. The present results suggest that a torque-based control ~~would always lead to a non-optimal~~ calibrated for flat terrain would lead to suboptimal power performance in ~~accelerating flows~~complex terrain, because the optimal local flow angles change, ~~while~~ whereas a torque controller keeps ~~the local flow angles constant. Whether including~~ them constant. However, this effect seems to be rather small. It remains to be investigated whether it is practically beneficial to include additional knowledge about the flow field in the control strategy~~and~~ , as well as adjusting the torque constant and pitch~~is beneficial overall remains to be investigated~~. It was shown that placing turbines in elevated regions with higher wind speeds ~~is beneficial for power performance~~improves power production. However, the degradation of the power coefficient leads to a reduced power output, not scaling with the speed-up over the hill cubed. The observed scaling in the simulations was closer to a quadratic trend, while theoretical considerations suggest a lower limit of the scaling close to the power of 1.5.

Appendix A: The effect of flow acceleration on the tangential induction

The simulation results show that the tangential induction is barely affected by the acceleration of the background flow, and major differences between the simulations can only be observed close to the root. At the root, the energy conversion process is different compared to the blade tips, because structural constraints require thick airfoils with a low lift-to-drag ratio, resulting in a flow that is significantly influenced by the drag of the airfoil. With this knowledge in mind, we now seek to investigate why the tangential induction is rather independent of flow acceleration in the outer region of the blade.

A control volume analysis of the conservation of angular momentum yields (Hansen, 2015)

$$dQ = r\, u_t^+ \, d\dot{m} = 4\pi\rho R^2 \mu^3 \lambda U_{\mathrm{Ref}}^2 (1-a) a' \, dr, \tag{A1}$$

with u_t^+ being the tangential velocity in the wake, which relates to the tangential induction as $a' = u_t^+/(2\omega r)$. Further we used for the mass flux $d\dot{m} = U_{\mathrm{Ref}}(1-a)2\pi r\, dr$. Note that $U_{\mathrm{Ref}}(1-a)$ only describes the velocity in the rotor plane, independently of what caused this velocity. Shifting the view towards the blade, the angular momentum can be calculated as

$$dQ = f_t N_B r \, dr, \tag{A2}$$

with the tangential force per spanlength f_t and the number of blades N_B. When taking a look at the force and flow vectors at each blade section, we now consciously ignore the drag of the airfoil yielding for the flow angle ϕ

$$\tan\phi = \frac{U_{\mathrm{Ref}}(1-a)}{\omega r(1+a')} = \frac{f_t}{f_n}, \tag{A3}$$

with the blade normal force per ~~spanlength~~ span length f_n. For the local thrust coefficient, we obtain

$$C_t = \frac{dT}{\frac{1}{2}\rho U_{\mathrm{Ref}}^2 \, dA} = \frac{dT}{\pi\rho U_{\mathrm{Ref}}^2 r \, dr} = \frac{f_n N_B}{\pi\rho U_{\mathrm{Ref}}^2 r}. \tag{A4}$$

Combining Eq. (A3) with Eq. (A4) yields for the tangential force

$$f_t = \frac{1-a}{1+a'} \frac{\pi R \rho U_{\mathrm{Ref}}^2 C_t}{\lambda N_B}, \tag{A5}$$

and by combining this with Eq. (A1) and Eq. (A2), we obtain

$$a'(1+a') = \frac{C_t}{4\lambda^2\mu^2}, \tag{A6}$$

which can be solved for the tangential induction yielding Eq. (24), showing that indeed, in regions where lift dominates the flow, the tangential induction only depends on $\frac{C_t}{\lambda^2}$, which a torque controller keeps constant.

The same result can be obtained in a vortex-theory framework without the need for a control-volume analysis, which is briefly outlined below. For an actuator disk with azimuthal constant loading, the induced tangential velocity due to the bound vortex ~~of strength Γ_B~~ system of strength $N_B\Gamma_B$ can be calculated from the definition of the circulation Γ~~as~~.

The circulation is generally written as

$$\Gamma = \oint u_s \, ds = 2\pi r u_{t,i}^+ = N_B\Gamma_B, \tag{A7}$$

with u_s being the tangential velocity along the curve s~~and~~. This yields for the bound vortex system

$$N_B\Gamma_B = 2\pi r u_{t,i}^+, \tag{A8}$$

with $u_{t,i}^+$ being the mean induced velocity behind the disk. Ahead of turbine, the mean induced velocity is $u_{t,i}^- = 0$ and therefore in the disk plane the induced velocity is

$$u_{t,i} = \frac{1}{2}\left(u_{t,i}^- + u_{t,i}^+\right) = \frac{N_B\Gamma_B}{4\pi r}. \tag{A9}$$

Based on the Kutta-Joukowsky condition, the axial force per ~~spanlength is calculated as $f_n = \rho\Gamma_B u_t$, yielding for the~~ span length f_n is calculated from

$$\begin{bmatrix} -f_n \\ -f_r \\ -f_t \end{bmatrix} = \rho \begin{bmatrix} u_n \\ u_r \\ u_t \end{bmatrix} \times \begin{bmatrix} 0 \\ \Gamma_B \\ 0 \end{bmatrix} = \begin{bmatrix} -\rho\Gamma_B u_t \\ 0 \\ \rho\Gamma_B u_n \end{bmatrix}, \tag{A10}$$

where we considered that our force vectors are defined as oriented in the opposite direction to the force acting on the flow. Further, u_n and u_r define the normal and radial velocity components, respectively, and f_r the radial force component. For the local C_t previously defined in Eq. (A4) we obtain

$$C_t = \frac{\Gamma_B u_t N_B}{U_{\mathrm{Ref}}^2 \pi r}. \tag{A11}$$

The total local tangential velocity relative to the blades can be calculated as the sum of the rotational component and the induced velocity

$$u_t = U_{\mathrm{Ref}}\lambda\mu + u_{t,i}. \tag{A12}$$

Using Eq. (A9) and introducing the non-dimensional bound circulation $\gamma = \frac{\omega N_B \Gamma_B}{\pi U_{\mathrm{Ref}}^2}$ yields

$$u_t = U_{\mathrm{Ref}} \lambda \mu \left(1 + a'\right), \tag{A13}$$

with the tangential induction defined as

$$a' = \frac{\gamma}{4\lambda^2 \mu^2}. \tag{A14}$$

Inserting this into Eq. (A11) yields

$$C_t = 4a' \lambda^2 \mu^2 \left(1 + a'\right), \tag{A15}$$

which is identical to the result from the momentum analysis in Eq. (A6).

Appendix B: Change of maximum C_P on an isolated hill

Zengler et al. (2025a) developed an engineering model based on momentum theory, which incorporates the effect of a streamwise acceleration of the background flow field. The modified equation for the power coefficient is

$$C_P = 4a(1-a)^2 + 4a(1-a)l\beta, \tag{B1}$$

with the term $l\beta$ being the product of a non-dimensional length scale l and a non-dimensional streamwise velocity gradient $\beta = \frac{D}{U_{\mathrm{Ref}}} \frac{dU}{dx}$. The length scale was assumed to be the distance behind the turbine, where the pressure in the wake equalizes with the surrounding pressure. It is often assumed that this point is around one diameter behind the turbine (Crespo et al., 1999; Dar and Porté-Agel, 2022), although research shows that its actual position depends on the thrust coefficient of the turbine and might be longer than one diameter (Liew et al., 2024). The undisturbed velocity behind the turbine where the background pressure equalizes is consequently

$$U_1 = U_{\mathrm{Ref}}(1 + l\beta). \tag{B2}$$

Now we consider a turbine located on a small hill. The speed-up ΔU over the hill is assumed to occur over a distance smaller than the distance over which the pressures in the wake of the turbine equalize. So we are speaking of a very local speed-up close to the turbine. As a consequence, the velocity U_1, at which the pressures equalize, is limited by this speed-up or rather speed-down behind the hill. With the notation introduced in the discussion of the speed-up factors in ~~See~~Sect. 4.3 with $U_{\mathrm{Ref,hill}}$ being the undisturbed velocity on top of the hill and $U_{\mathrm{Ref,flat}}$ being the undisturbed velocity around the hill, this means that $U_1 = U_{\mathrm{Ref,flat}}$. Expressing it in terms of the velocity on top of the hill, where the turbine is located yields

$$U_1 = U_{\mathrm{Ref,hill}} \left(1 - \frac{\Delta U}{1 + \Delta U}\right). \tag{B3}$$

Comparing this expression with Eq. (B2), we see that

$$l\beta = -\frac{\Delta U}{1 + \Delta U}. \tag{B4}$$

Next, we ask what the optimal performance a turbine can achieve is based on these considerations. Keeping the $l\beta$-notation for the sake of brevity, the induction, which maximizes C_P is found by differentiation of Eq. (B1) to be

$$a_{\mathrm{opt}} = \frac{2}{3} + \frac{1}{3} l\beta - \frac{1}{3}\sqrt{1 + l\beta + l^2\beta^2}. \tag{B5}$$

For $l\beta = 0$, one obaines $a_{\mathrm{opt}} = \frac{1}{3}$, which is the classical result from momentum theory. ~~$C_{P,\mathrm{max}}$~~ $C_{P\mathrm{max}}$ can be determined by inserting the optimal induction into the equation for the power coefficient (B1)~~.~~, which yields

$$C_{P\mathrm{max}} = \frac{8}{27}\left(1 - l^3\beta^3 + (1 + l\beta + l^2\beta^2)^{1.5}\right) + \frac{4}{9}(l\beta - l^2\beta^2). \tag{B6}$$

This result is, based on the previous argument, only valid for the case, where the undisturbed velocity behind the turbine immediately recovers to the velocity around the hill before the pressure equalizes with the surrounding flow.

Code and data availability. EllipSys3D used for the simulations is a proprietary software developed at DTU Wind and Energy Systems and distributed under licence.

Author contributions. CPZ: conceptualization, data curation, formal analysis, investigation, methodology, visualization, writing (original draft preparation) MG: conceptualization, methodology, formal analysis, supervision, writing (review and editing) NT: conceptualization, methodology, supervision, writing (review and editing)

Competing interests. The contact author has declared that none of the authors has any competing interests.

Acknowledgements. This work has been partially supported by the EU project MERIDIONAL with grant agreement No. 101084216. We also gratefully acknowledge the computational and data resources provided on the Sophia HPC Cluster at the Technical University of Denmark (https://doi.org/10.57940/FAFC-6M81).

References

Abbas, N. J., Zalkind, D. S., Pao, L., and Wright, A.: A reference open-source controller for fixed and floating offshore wind turbines, Wind Energy Science, 7, 53–73, https://doi.org/10.5194/wes-7-53-2022, 2022.

Bak, C., Zahle, F., Bitsche, R., KIm, T., Yde, A., Henriksen, L. C., Natarajan, A., and Hansen, M. H.: Description of the DTU 10 MW Reference Wind Turbine, Tech. Rep. DTU Wind Energy Report-I-0092, DTU Wind Energy, Roskilde, Denmark, 2013.

Bianchi, F. D., Mantz, R. J., and Battista, H. d., eds.: Wind Turbine Control Systems: Principles, Modelling and Gain Scheduling Design, Advances in Industrial Control, Springer London, London, ISBN 978-1-84628-492-2 978-1-84628-493-9, https://doi.org/10.1007/1-84628-493-7, 2007.

Bossanyi, E. A.: The Design of closed loop controllers for wind turbines, Wind Energy, 3, 149–163, https://doi.org/10.1002/we.34, 2000.

Cai, T., Cheng, S., Segalini, A., and Chamorro, L. P.: Local topography-induced pressure gradient effects on the wake and power output of a model wind turbine, Theoretical and Applied Mechanics Letters, 11, 100 297, https://doi.org/10.1016/j.taml.2021.100297, 2021.

Calaf, M., Meneveau, C., and Meyers, J.: Large eddy simulation study of fully developed wind-turbine array boundary layers, Physics of Fluids, 22, 015 110, https://doi.org/10.1063/1.3291077, 2010.

Creaby, J., Li, Y., and Seem, J. E.: Maximizing Wind Turbine Energy Capture Using Multivariable Extremum Seeking Control, Wind Engineering, 33, 361–387, https://doi.org/10.1260/030952409789685753, 2009.

Crespo, A., Hernández, J., and Frandsen, S.: Survey of Modelling Methods for Wind Turbine Wakes and Wind Farms, Wind Energy, 2, 1–24, https://doi.org/10.1002/(SICI)1099-1824(199901/03)2:1<1::AID-WE16>3.0.CO;2-7, 1999.

Dar, A. S. and Porté-Agel, F.: An Analytical Model for Wind Turbine Wakes under Pressure Gradient, Energies, 2022, 5345, https://doi.org/10.3390/en15155345, 2022.

Dar, A. S., Gertler, A. S., and Porté-Agel, F.: An experimental and analytical study of wind turbine wakes under pressure gradient, Physics of Fluids, 35, 045 140, https://doi.org/10.1063/5.0145043, 2023.

Dar, A. S., Revaz, T., and Porté-Agel, F.: A model for the effect of pressure gradient on the induction and power of wind turbines, Physics of Fluids, 37, 085 128, https://doi.org/10.1063/5.0277577, 2025.

Dar, A. S., Revaz, T., and Porté-Agel, F.: Theoretical efficiency of a wind turbine in non-uniform base flow: Revisiting the Betz–Joukowsky limit, Physics of Fluids, 38, 041 702, https://doi.org/10.1063/5.0300485, 2026.

Elliot, D. L. and Cadogan, J. B.: Effects of Wind Shear and Turbulence on Wind Turbine Power Curves, in: European Community Wind Energy Conference. Proceedings of an International Conference (eur 13251), edited by Palz, W., pp. 79–83, H.S. Stephens, Madrid, Spain, ISBN 978-0-9510271-8-9, 1990.

Hansen, M. H. and Henriksen, L. C.: Basic DTU Wind Energy controller, Tech. Rep. E-0028, DTU Wind Energy, Roskilde, Denmark, 2013.

Hansen, M. O. L.: Aerodynamics of wind turbines, Routledge, London, New York, 3 edn., ISBN 978-1-138-77507-7, 2015.

Johnson, K. E., Pao, L. Y., Balas, M. J., and Fingerish, L. J.: Control of variable-speed wind turbines: standard and adaptive techniques for maximizing energy capture, IEEE Control Systems, 26, 70–81, https://doi.org/10.1109/mcs.2006.1636311, 2006.

Jonkman, B., Platt, A., Mudafort, R. M., Slaughter, D., Branlard, E., Wang, L., Ross, H., Sprague, M., HaymanConsulting, Davies, R., jjonkman, Chetan, M., cortadocodes, Hall, M., Vijayakumar, G., Buhl, M., reos rcrozier, Russell9798, Bergua, R., Bortolotti, P., Gupta, A., Ananthan, S., JustinPorter88, Rood, J., rdamiani, nrmendoza, Barter, G., Bhuiyan, F. H., sinolonghai, and Sakievich, P.: OpenFAST/openfast: Release v5.0.0, https://doi.org/10.5281/ZENODO.18992186, 2026.

Jonkman, J., Butterfield, S., Musial, W., and Scott, G.: Definition of a 5-MW Reference Wind Turbine for Offshore System Development, Tech. Rep. NREL/TP-500-38060, 947422, National Renewable Energy Laboratory, https://doi.org/10.2172/947422, 2009.

Kolmogorov, D. K., Shen, W. Z., Sørensen, N. N., and Sørensen, J. N.: Fully Consistent SIMPLE-Like Algorithms on Collocated Grids, Numerical Heat Transfer, Part B: Fundamentals, 67, 101–123, https://doi.org/10.1080/10407790.2014.949583, 2015.

Larsen, T. J. and Hansen, A. M.: How 2 HAWC2, the user's manual, Tech. Rep. Risø-R-1597, Department of Wind and Energy Systems, Roskilde, Denmark, 2025.

Liew, J., Heck, K. S., and Howland, M. F.: Unified momentum model for rotor aerodynamics across operating regimes, Nature Communications, 15, 6658, https://doi.org/10.1038/s41467-024-50756-5, 2024.

Liu, L. and Stevens, R. J. A. M.: Effects of Two-Dimensional Steep Hills on the Performance of Wind Turbines and Wind Farms, Boundary-Layer Meteorology, 176, 251–269, https://doi.org/10.5194/wes-7-1527-2022, 2020.

Meyers, J. and Meneveau, C.: Large Eddy Simulations of Large Wind-Turbine Arrays in the Atmospheric Boundary Layer, in: 48th AIAA Aerospace Sciences Meeting Including the New Horizons Forum and Aerospace Exposition, American Institute of Aeronautics and Astronautics, Orlando, Florida, ISBN 978-1-60086-959-4, https://doi.org/10.2514/6.2010-827, 2010.

Michelsen, J.: Basis3D - a Platform for Development of Multiblock PDE Solvers, Tech. rep., Technical University of Denmark, 1992.

Michelsen, J.: Block structured multigrid solution of 2D and 3D elliptic PDE's, Tech. rep., Technical University of Denmark, 1994.

Mikkelsen, R.: Actuator disc methods applied to wind turbines, Ph.D. thesis, Technical University of Denmark, Lyngby, Denmark, 2004.

Mishra, A., Arya, N., and Bhattacharya, A.: Wake steering of wind turbine in the presence of a two-dimensional hill, Physics of Fluids, 36, 045 125, https://doi.org/10.1063/5.0185842, 2024.

Pao, L. Y. and Johnson, K. E.: Control of Wind Turbines, IEEE Control Systems, 31, 44–62, https://doi.org/10.1109/mcs.2010.939962, 2011.

Prospathopoulos, J. M., Cabezon, D., Politis, E. S., Chaviaropoulos, P. K., Rados, K. G., Schepers, J. G., Hansen, K., and Barthelmie, R. J.: Simulation of Wind Farms in Flat and Complex Terrain using CFD, in: Torque 2010: The science of making torque from wind, pp. 359–370, read_Status: New Read_Status_Date: 2023-12-21T09:34:55.799Z, 2010.

Revaz, T. and Porté-Agel, F.: Effect of hills on wind turbine flow and power efficiency: A large-eddy simulation study, Physics of Fluids, 36, 095 180, https://doi.org/10.1063/5.0226544, 2024.

Réthoré, P.-E., van der laan, M. P., Troldborg, N., Zahle, F., and Sørensen, N. N.: Verification and validation of an actuator disc model, Wind Energy, 17, 919–937, https://doi.org/10.1002/we.1607, 2014.

Sørensen, N. N.: General purpose flow solver applied to flow over hills, phd, Risø National Laboratory, 1995.

Sørensen, N. N.: EllipSys2D/3D User Manual, Tech. rep., DTU Wind Energy, Roskilde, Denmark, https://ellipsys.pages.windenergy.dtu.dk/docs/main.html, 2018.

Sørensen, N. N., Bechmann, A., Johansen, J., Myllerup, L., Botha, P., Vinther, S., and Nielsen, B. S.: Identification of severe wind conditions using a Reynolds Averaged Navier-Stokes solver, Journal of Physics: Conference Series, 75, 012 053, https://doi.org/10.1088/1742-6596/75/1/012053, 2007.

Troen, I. and Petersen, E. L.: European wind atlas, Risø National Laboratory, Roskilde, Denmark, 1989.

Troldborg, N., Sørensen, N., Réthoré, P.-E., and van der Laan, M. P.: A consistent method for finite volume discretization of body forces on collocated grids applied to flow through an actuator disk, Computers & Fluids, 119, 197–203, https://doi.org/10.1016/j.compfluid.2015.06.028, 2015.

Troldborg, N., Andersen, S. J., Hodgson, E. L., and Meyer Forsting, A.: Brief communication: How does complex terrain change the power curve of a wind turbine?, Wind Energy Science, 7, 1527–1532, https://doi.org/10.5194/wes-7-1527-2022, 2022.

van der Laan, M. P., Sørensen, N. N., Réthoré, P.-E., Mann, J., Kelly, M. C., and Troldborg, N.: The k-ϵ-fp model applied to double wind turbine wakes using different actuator disk force methods, Wind Energy, 18, 2223–2240, https://doi.org/10.1002/we.1816, 2014.

van der Laan, M. P., Sørensen, N. N., Réthoré, P.-E., Mann, J., Kelly, M. C., Troldborg, N., Hansen, K. S., and Murcia, J. P.: The k-ϵ-fP model applied to wind farms, Wind Energy, 18, 2065–2084, https://doi.org/10.1002/we.1804, 2015a.

van der Laan, M. P., Sørensen, N. N., Réthoré, P.-E., Mann, J., Kelly, M. C., Troldborg, N., Schepers, J. G., and Machefaux, E.: An improved k - ϵ model applied to a wind turbine wake in atmospheric turbulence, Wind Energy, 18, 889–907, https://doi.org/10.1002/we.1736, 2015b.

van der Laan, M. P., Andersen, S., Kelly, M., and Baungaard, M.: Fluid scaling laws of idealized wind farm simulations, Journal of Physics: Conference Series, 1618, 062 018, https://doi.org/10.1088/1742-6596/1618/6/062018, 2020.

Wagner, R., Courtney, M., Gottschall, J., and Lindelöw-Marsden, P.: Accounting for the speed shear in wind turbine power performance measurement, Wind Energy, 14, 993–1004, https://doi.org/10.1002/we.509, 2011.

Wu, Y.-T. and Porté-Agel, F.: Modeling turbine wakes and power losses within a wind farm using LES: An application to the Horns Rev offshore wind farm, Renewable Energy, 75, 945–955, https://doi.org/10.1016/j.renene.2014.06.019, 2015.

Zengler, C. P., Troldborg, N., and Gaunaa, M.: Is the free wind speed sufficient to determine aerodynamic turbine performance in complex terrain?, Journal of Physics: Conference Series, 2767, 092 049, https://doi.org/10.1088/1742-6596/2767/9/092049, 2024.

Zengler, C. P., Troldborg, N., and Gaunaa, M.: Modeling the influence of streamwise flow field acceleration on the aerodynamic performance of an actuator disk, Wind Energy Science, 10, 1485–1497, https://doi.org/10.5194/wes-10-1485-2025, 2025a.

Zengler, C. P., Troldborg, N., and Gaunaa, M.: Predicting the impact of flow field acceleration on wind turbine performance in complex terrain and wind farms, Journal of Physics: Conference Series, 3016, 012 003, https://doi.org/10.1088/1742-6596/3016/1/012003, 2025b.

Øye, S.: Flex4 simulation of wind turbine dynamics, in: Proc. of 28th IEA Meeting of Experts Concerning State of the Art of Aeroelastic Codes for Wind Turbine Calculations, pp. 71–76, IEA, Lyngby, Denmark, 1996.